A New Class of Complexes Possessing Cofacially-Oriented, Planar, Metal-Containing Subunits. Synthesis, Characterization, and Reactivity of $[(MoO_2)_2(\mu\text{-}O)]^{2+}$-Linked, Catechol-Functionalized, Tetraazamacrocyclic and Salicylideneamine Complexes

Steven M. Malinak, Dell T. Rosa, and Dimitri Coucouvanis*

Department of Chemistry, The University of Michigan, Ann Arbor, Michigan 48109-1055

Received December 22, 1997

A new synthetic route to molecules that contain cofacially oriented, $[Mo_2O_5]^{2+}$-bridged bis(catecholate) dianions is described. This synthesis has been useful in the preparation of supermolecular molecules containing catechol-functionalized, metalated macrocyclic $[M^{II}(TAD(OH)_2)]$ (M = Co, Ni) and SALPHEN $[M^{II}(R_2R'_2SALPHEN-(OH)_2)]$ (M = H_2, Mn, Fe, Co, Ni, Cu) ligands. Of the former, the $(Bu_4N)_2[Mo_2O_5[Ni(TAD(O)_2)]_2]$ (**7**) complex has been structurally characterized. The complex crystallizes in the triclinic space group $P\bar{1}$ with unit cell dimensions a = 12.324(3) Å, b = 17.740(4) Å, c = 20.920(4) Å, α = 108.79(3)°, β = 98.20(3)°, and γ = 103.12(3)°. The nearly-planar macrocyclic ligands are essentially parallel, with a dihedral angle of 6.5(2)°. The Ni(1)--Ni(2) separation in the anion is 3.938 Å. The structure of $(Bu_4N)_2[Mo_2O_5[Cu(EtO_2H_2SALPHEN(O)_2)]_2]$ (**19**) has also been determined. This complex crystallizes in the monoclinic space group $P2_1/c$, with unit cell dimensions a = 20.821(4) Å, b = 23.133(5) Å, c = 20.056(4) Å, and β = 117.71(3)°. The Cu(1)--Cu(2) separation is 4.110 Å, and the dihedral angle between SALPHEN "planes" is approximately 9.7(1)°. Analytical and spectroscopic properties are provided. Reactions of these molecules with oxidants and strongly coordinating ligands are presented. The ability of the Fe^{II} and Co^{II} analogues of **19** to bind ligands such as O^{2-} or S^{2-} and O_2, respectively, in the "pocket" of the complex is described, and the products have been characterized. The synthesis and characterization of the unique "mixed catecholate" complexes $(Bu_4N)_2[Mo_2O_5(D^tBC)(M^{II}(^tBu_4SALPHEN-(O)_2))]$ (M = H_2, Fe, Co, Ni, Cu) is described, and comparisons between these latter systems and the bis(M^{II}-SALPHEN-catecholate) complexes are provided.

Introduction

The coordination chemistry of catechol-functionalized macrocyclic ligands has been explored recently in this laboratory. These ligands include (a) the tetraazacyclotetradecamacrocyclic ligand $H_2TAD(OH)_2$ (Figure 1A)[1] and (b) derivatives of salicylideneamine obtained by condensation of 4,5-diaminocatechol and various salicylaldehydes, $H_2(R_2R'_2SALPHEN(OH)_2)$ (Figure 1B).[2] The catechol-functionalized macrocyclic or SALPHEN complexes form metal complexes which in turn are effective as ligands in the synthesis of multinuclear supermolecules. Various $M[M'(TAD\text{-}(O)_2)]_2^{2-}$ complexes (M = $[Mo_2(\mu\text{-}S)_2(O)_2]^{2+}$, VO^{2+}, Co^{2+}, Cu^{2+}, Zn^{2+}; M′ = Co^{2+}, Ni^{2+}) have been obtained,[3] and the structures of some of the parent metalated macrocyclic catechols and derivatives are now available.[1,3] The use of the $H_2TAD(OH)_2$ and $H_2(R_2R'_2$-SALPHEN$(OH)_2$) multifunctional ligands in the synthesis of a new class of molecules with cofacially oriented, planar, macrocyclic or SALPHEN complexes bridged by the $[(MoO_2)_2(\mu\text{-}O)]^{2+}$ unit will be the subject of this paper. Interest in these compounds derives from (a) the unique properties of the previously studied[4,5] cofacial porphyrin complexes and (b) the redox characteristics of the metallocatecholate ligands and their possible involvement in multielectron reductions.

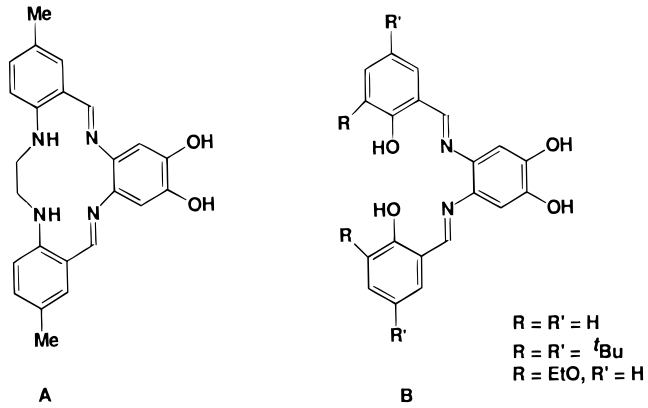

Figure 1. Macrocyclic- and SALPHEN-catechol ligands employed in this study.

The synthesis, structural characterization, and reactivity characteristics of complexes composed of cofacially oriented

(1) (a) Jonasdottir, S. G.; Kim, C. G.; Kampf, J.; Coucouvanis, D. *Inorg. Chim. Acta* **1996**, *243*, 255. (b) Coucouvanis, D.; Jonasdottir, S. G.; Christodoulou, D.; Kim, C.-G., Kampf, J. W. *Inorg. Chem.* **1993**, *32*, 2987.

(2) Rosa, D. T.; Reynolds R. A., III; Malinak, S. M.; Baumann, T. F.; Coucouvanis, D. To be reported separately.

(3) (a) Jonasdottir, S. G.; Kim, C. G.; Coucouvanis, D. *Inorg. Chem.* **1993**, *32*, 3591. (b) Jonasdottir, S. G. Ph.D. Thesis, The University of Michigan, Ann Arbor, MI, 1994.

(4) Collman, J. P.; Wagenknecht, P. S.; Hutchison, J. E. *Angew. Chem., Int. Ed. Engl.* **1994**, *33*, 1537 and references therein.

(5) (a) Fillers, J. P.; Ravichandran, K. G.; Abdalmuhdi, I.; Tulinsky, A.; Chang, C. K. *J. Am. Chem. Soc.* **1986**, *108*, 417. (b) Eaton, S. S.; Eaton, G. R.; Chang, C. K. *J. Am. Chem. Soc.* **1985**, *107*, 3177. (c) Chang, C. K.; Liu, H. Y.; Abdalmuhdi, I. *J. Am. Chem. Soc.* **1984**, *106*, 2725. (d) Chang, C. K.; Tulinsky, A.; Hatada, M. H. *J. Am. Chem. Soc.* **1980**, *102*, 7116.

S0020-1669(97)01591-7 CCC: $15.00
Published on Web 03/04/1998

metal−porphyrins bridged by organic spacers have been the subject of elegant studies by Collman[4] and others.[5] Studies on these complexes have shown that the cofacially oriented macrocycles can be functional in the bimetallic activation of small molecules or ions such as O_2, NH_3, and H^+. The specific reactions depend on the identity of the porphyrin-bound metal ions and include the activation and oxidation of NH_3 and N_2H_2 by cofacially oriented Ru−porphyrins,[6] the reduction of H^+ by the Ru− and Os−diporphyrins,[7] and the reduction of O_2 by analogous Co−/M−diporphyrins (M = Co;[4,8] M = Ti, Ga, In, Lu, Sc[9]).

The ability of the catecholate subunits in the cofacial macrocyclic or SALPHEN $[Mo_2O_5]^{2+}$ derivatives to undergo relatively facile oxidation may increase the capacity of these molecules to deliver electrons in the multielectron reduction of substrates. It is interesting to note that in biological systems such as the ribonucleotide reductase,[10] photosystem II,[11] and galactose oxidase[12] enzymes, in addition to reducing metal centers, reducing equivalents sometimes are obtained from tyrosine residues with generation of tyrosyl radicals.

The synthesis of the macrocyclic-catechol $[Mo_2O_5]^{2+}$ derivatives was inspired by the known $[Mo_2O_5(3,5\text{-}R_2\text{catecholate})_2]^{2-}$ (R = H[13] or ^{t}Bu[14]) and $[Mo_2O_5(\text{phenanthrenequinone})_2]$[15] complexes. The structures of these molecules are known[13,14a,15] and show the two catecholate/semiquinone ligands in a cofacial orientation. Herein is reported the detailed synthesis and reactivities of a variety of $[Mo_2O_5(M(TAD\text{-}(O)_2))_2]^{2-}$ and $[Mo_2O_5(M(R_2R'_2SALPHEN(O)_2))_2]^{2-}$ complexes. Portions of this work have been published in preliminary fashion.[16]

Experimental Section

General Considerations. All manipulations were performed under an inert atmosphere using standard glovebox and Schlenk techniques, unless otherwise noted. Solvents were distilled under N_2 from the appropriate drying agents (THF, diethyl ether, toluene from sodium/benzophenone; CH_2Cl_2, hexanes, pyridine from CaH_2; CH_3CN from B_2O_3; methanol from $MgSO_4$) and/or stored over 3 Å molecular sieves (acetone, absolute ethanol, and distilled pyridine) and thoroughly degassed with N_2 prior to use. Reagent grade chemicals were purchased from Aldrich Chemical Co. (96% CH_3NO_2, 95% $Fe(OAc)_2$, $Mn(OAc)_2{\cdot}4H_2O$, $Co(OAc)_2{\cdot}4H_2O$, $Ni(OAc)_2{\cdot}4H_2O$, $Na_2MoO_4{\cdot}2H_2O$, Bu_4NBr, $Et_4N(CN)$, $Et_4N(SCN)$, 3,5-di-*tert*-butylsalicylaldehyde, 3-ethoxysalicylaldehyde, tetrachlorocatechol, 3,5-di-*tert*-butylcatechol, benzyl trisulfide, 1.0 M $Bu_4N(OH)$ in methanol), Fisher $(Cu(OAc)_2{\cdot}2H_2O)$, and Matheson (dry O_2) and used without further purification.

Abbreviations used: CAT (catecholate), Cl_4-CAT (tetrachlorocatecholate), D^{t}BC (3,5-di-*tert*-butylcatecholate), pyH^+ (pyridinium), $[M^{II}(TAD(OH)_2)]$ ((2,3-ethylene-5,6:13,14-di(5′-MeBzo)-9,10-(4′,5′-$(OH)_2$Bzo)-[14]-1,4,8,11-[N_4]-7,12-dienoato)M^{II}, or metalated macrocyclic catechol), $[M^{II}(R_2R'_2SALPHEN(OH)_2)]$ ((*N*,*N*′-bis(3-R-5-R′-salicylidene)-4,5-dihydroxyphenylenediaminato)M^{II}, or metalated SALPHEN catechol), $[M^{II}(R_2R'_2SALPHENSQ(O)(OH))]$ (metalated SALPHEN semiquinone), MIDA ((methylimino)diacetate), Fc^+ (ferrocenium cation).

Physical Measurements. Infrared spectra (CsI or KBr pellets) were obtained using a Nicolet 740 FT-IR spectrometer (far-IR: 500−150 cm^{-1}) or a 5DXB FT-IR spectrometer (mid-IR: 4000−400 cm^{-1}). Electronic spectra were obtained with a Cary 1E spectrophotometer using a 1 mm quartz cell. Magnetic data were obtained using a Quantum Design SQUID magnetometer. Proton NMR spectra were recorded on Bruker 300 or 360 MHZ pulse FX NMR spectrometers in acetone-d_6. Elemental analyses were performed by the analytical services laboratory at the University of Michigan. Analysis samples were routinely kept under dynamic vacuum for 12 h before submission. Mass spectra were obtained either from in-house facilities (fast atom bombardment) or the Protein and Carbohydrate Structure Facility (Medical Science, electron spray) at the University of Michigan. EPR spectra were obtained and integrated to determine concentration according to previously developed techniques.[17]

Preparation of Compounds. $[M^{II}(TAD(OH)_2)]$ (M = Co, Ni) was prepared as described.[1] The syntheses of $(Bu_4N)_4[Mo_8O_{26}]$ and $(Bu_4N)_2[Mo_2O_7]$ have been reported previously.[18]

[H$_2$(^{t}Bu$_4$SALPHEN)−(OH)$_2$]·ether. 4,5-Diaminocatechol hydrobromide[2] (2.0 g, 9.0 mmol) was dissolved in 200 mL of methanol. A slight excess of pyridine (1.0 mL) was added to neutralize the HBr. 3,5-Di-*tert*-butylsalicylaldehyde (4.24 g, 18.0 mmol) was then added in one portion. The solution was refluxed overnight, turning a deep yellow color within the first few hours. The solvent was then removed *en vacuo*, and the residue was taken up in diethyl ether. The resulting slurry was then filtered in air over a pad of Celite to remove pyHBr. The filtrate was again taken to dryness, and the resulting yellow orange powder was dissolved in a minimum amount of warm hexanes. This latter solution was placed in the freezer, and after overnight standing, a yellow crystalline solid precipitates. The solid was obtained by filtration and dried under vacuum. Yield: ∼4−5 g (70−85%). Elemental analysis and the ^{1}H NMR spectrum support the formulation as a monoetherate. Anal. Calcd for $C_{40}H_{56}N_2O_5$: C, 74.25; H, 9.05; N, 4.33. Found: C, 73.77; H, 9.14; N, 4.29. NMR (δ, ppm): 1.90 (triplet, C*H*$_3$CH$_2$− from ether); 1.28, 1.30 (singlets from *tert*-butyl groups); 3.45 (quadruplet, CH$_3$C*H*$_2$− from ether); 6.88 (singlet, ring proton on catechol); 7.23, 7.43 (*meta*-coupled doublets from ring protons on phenol); 8.62 (singlet, N=C*H*). Mid-IR (cm^{-1}, KBr disk): ν(C=N), 1661 (vs). Electronic spectrum [nm (ϵ, M^{-1} cm^{-1}), CH_3CN solution]: 386 (sh), 356 (24 000), 301 (sh), 279 (27 000).

[M^{II}(^{t}Bu$_4$SALPHEN(OH)$_2$)] (M = Co or Ni). [H$_2$(^{t}Bu$_4$SALPHEN-(OH)$_2$]·ether (2.0 g, 3.1 mmol) was dissolved in 75 mL of MeOH. $M(OAc)_2{\cdot}4H_2O$ (2 equiv) was then added in one portion. The solution slowly became deep red. After approximately 45 min of stirring, precipitation of a red microcrystalline solid began. The reaction was stirred for 1 h and filtered. The collected solid was washed well with small amounts of cold methanol and dried under vacuum. Typical yields are approximately 1.2 g (60%). A second crop of powder can be isolated by reducing the solvent volume from the filtrate to approximately 20 mL.

[Co(^{t}Bu$_4$SALPHEN(OH)$_2$)]. Anal. Calcd for $C_{36}H_{46}N_2O_4Co$: C, 68.76; H, 7.37; N, 4.45. Found: C, 68.55; H, 7.49; N, 4.29. Mid-IR (cm^{-1}, KBr disk): ν(C=N), 1661 (vs). Electronic spectrum [nm (ϵ, M^{-1} cm^{-1}), CH_2Cl_2 solution]: 588 (sh), 531 (sh), 436 (sh), 408 (34 000), 385 (sh), 360 (26 000), 341 (sh), 315 (sh), 305 (29 000).

[Ni(^{t}Bu$_4$SALPHEN(OH)$_2$)]. Anal. Calcd for $C_{36}H_{46}N_2O_4Ni$: C, 68.76; H, 7.38; N, 4.46. Found: C, 68.50; H, 7.53; N, 4.65. Mid-

(6) Collman, J. P.; Hutchison, J. E.; Ennis, M. S., Lopez, M. A.; Guilard, R. *J. Am. Chem. Soc.* **1992**, *114*, 8074.
(7) Collman, J. P.; Ha, Y.; Wagenknecht, P. S.; Lopez, M.-A.; Guilard, R. *J. Am. Chem. Soc.* **1993**, *115*, 9080.
(8) Collman, J. P.; Denisevich, P.; Konai, Y.; Marrocco, M.; Koval, C.; Anson, F. C. *J. Am. Chem. Soc.* **1980**, *102*, 6027.
(9) Guilard, R.; Brandes, S.; Tardieux, C.; Tabard, A.; L'Her, M.; Miry, C.; Gouerec, P.; Knop, Y.; Collman, J. P. *J. Am. Chem. Soc.* **1995**, *117*, 11721.
(10) Gerfen, G. J.; Bellew, B. F.; Bollinger, J. M.; Stubbe, J.; Griffin, R. G.; Singel, D. J. *J. Am. Chem. Soc.* **1993**, *115*, 6420.
(11) (a) Galli, C.; Atta, M.; Anderson, K. K.; Graslund, A.; Brudvig, G. W. *J. Am. Chem. Soc.* **1995**, *117*, 740. (b) Hoganson, C. W.; Babcock, G. T. *Biochemistry* **1992**, *31*, 11874.
(12) (a) Whittaker, M. M.; Whittaker, J. W. *J. Biol. Chem.* **1988**, *263*, 6074. (b) Winkler, M. E.; Bereman, R. D. *J. Am. Chem. Soc.* **1980**, *102*, 6244.
(13) Atovmyan, L. O.; Tkachev, V. V.; Shiskova, T. G. *Dokl. Akad. Nauk SSSR* **1972**, *205*, 609.
(14) (a) Pierpont, C. G.; Buchanan, R. M. *Inorg. Chem.* **1982**, *21*, 652. (b) Wilshire, J. P.; Leon, L.; Bosserman, P.; Sawyer, D. T. *Molybdenum Chemistry of Biological Significance*; Newton, W. E., Otsuka, S., Eds.; Plenum Press: New York, 1980; p 327. (c) Wilshire, J. P.; Leon, L.; Bosserman, P.; Sawyer, D. T. *J. Am. Chem. Soc.* **1979**, *101*, 3379.
(15) Pierpont, C. G.; Buchanan, R. M. *J. Am. Chem. Soc.* **1975**, *97*, 6450.
(16) Malinak, S. M.; Coucouvanis, D. *Inorg. Chem.* **1996**, *35*, 4810.
(17) Hearshen, D. O.; Hagen, W. R.; Sands, R. H.; Grande, H. J.; Dunham, W. R. *J. Magn. Reson.* **1986**, *69*, 440 and references therein.
(18) Filowitz, R. K.; Ho, C.; Klemperer, W. G.; Shum, W. *Inorg. Chem.* **1979**, *18*, 93.

IR (cm^{-1}, KBr disk): ν(C═N), 1661 (vs). Electronic spectrum [nm (ϵ, M^{-1} cm^{-1}), CH_2Cl_2 solution]: 493 (11 000), 471 (sh), 401(sh), 385 (30 000), 373 (sh), 298 (19 000).

[H_2(EtO$_2$H$_2$SALPHEN(OH)$_2$)]·pyHBr. 4,5-Diaminocatechol hydrobromide (2.0 g, 9.0 mmol) was dissolved in 20 mL of ethanol. A slight excess of pyridine was added to neutralize the HBr. In a separate flask, 3-ethoxysalicylaldehyde (3.0 g, 18 mmol) was dissolved in 20 mL of ethanol. The solutions were then combined with stirring. The solution developed an intense orange color immediately. A bright orange powder began to precipitate within 20 min. Stirring was continued for 2 h, after which the reaction was filtered to remove the orange solid, which was subsequently washed well with ether and dried under vacuum. Elemental analysis and the ^{1}H NMR spectrum both support the formulation as a coprecipitation of the ligand with pyridinium bromide. The reaction yield was 70%. Anal. Calcd for $C_{29}H_{30}N_3O_6Br$: C, 58.38; H, 5.08; N, 7.05. Found: C, 58.08; H, 5.29; N, 6.97. NMR (δ, ppm): 1.34 (triplet, C*H*$_3$CH$_2$− from ethoxy); 4.05 (quadruplet, CH$_3$C*H*$_2$− from ethoxy); 7.00 (singlet, ring proton on catechol); 7.23 (doublet), 7.08 (doublet), 6.90 (doublet of doublets) from ring protons on phenol; 8.79 (singlet, N═C*H*). Pyridinium appears at 7.96 (triplet), 8.46 (triplet), and 8.88 (doublet). Mid-IR (cm^{-1}, KBr disk): ν(N−H from pyH$^+$), 3096 (m); ν(C═N), 1615 (vs). Electronic spectrum [nm (ϵ, M^{-1} cm^{-1}), CH_3CN solution]: 449 (sh), 380 (sh), 350 (22000), 326 (sh), 278 (24000), 263 (sh), 258 (sh).

(Bu$_4$N)$_2$[[(MIDA)MoO$_2$]$_2$(μ-O)]. An amount of (Bu$_4$N)$_2$[Mo$_2$O$_7$] (0.3 g, 0.38 mmol) was added to a slurry of (methylimino)diacetic acid (0.11 g, 0.75 mmol) in 20 mL of CH_3CN. The acid slowly went into solution as the reaction occurred. After being stirred for 2 h, the solution was filtered. Diethyl ether (100 mL) was carefully added and allowed to diffuse into the filtrate. Upon standing overnight, 0.2 g (50%) of off-white crystals were obtained by filtration. Anal. Calcd for $C_{42}H_{86}N_4O_{13}Mo_2$ (MW = 1047.20): C, 48.17; H, 8.29; N, 5.35. Found: C, 48.20; H, 8.02; N, 5.28. Mass spectrum (FAB−, *m/e*): M$^-$ ([(Bu$_4$N)[Mo$_2$O$_5$(MIDA)$_2$]$^-$) = 806; M$^-$ ([Mo$_2$O$_5$(MIDA)$_2$]$^-$) = 563. Mid-IR (cm^{-1}, CsI disks): ν(C═O, free), 1680 (vs); ν(C═O, asym), 1655 (vs); ν(C═O, sym), 1365 (s); ν(Mo═O), 935 (vs), 903 (vs), 885 (vs); ν(Mo−O−Mo), 770 (vs). Far-IR (cm^{-1}, CsI disks): 268 (vs), 325 (w), 335 (w), 368 (m), 372 (sh), 387 (sh), 412 (m), 471 (vs), 475 (sh).

(Bu$_4$N)$_2$[Mo$_2$O$_5$(catecholate)$_2$] (catecholate = 3,5-Di-*tert*-butylcatecholate (1), 3,4,5,6-Tetrachlorocatecholate (2), or 3,4,5,6-Tetrahydrocatecholate (3)). An amount of the catechol (2 equiv) was added to a stirring solution (50 mL) of 0.65 g (0.82 mmol) of (Bu$_4$N)$_2$[Mo$_2$O$_7$] in CH_2Cl_2. The solution immediately became pale orange. Stirring was continued for an additional 3 h. The solution was then filtered, and diethyl ether (150 mL) was added and allowed to slowly diffuse into the filtrate. Orange crystals deposited and were obtained by filtration in 90% yield after overnight standing. Analytical and spectroscopic data for **2** and **3** are provided in the Supporting Information.

(Bu$_4$N)$_2$[Mo$_2$O$_5$(D^{t}BC)$_2$] (1). The spectroscopy and physical properties of this complex, previously obtained by a different synthetic route,[14] were consistent with those reported. Anal. Calcd for $C_{60}H_{112}N_2O_9Mo_2$: C, 60.17; H, 9.45; N, 2.34. Found: C, 60.07; H, 9.11; N, 2.33. NMR (δ, ppm): 1.14 (singlet, *tert*-butyl group); 1.27 (singlet, *tert*-butyl group); 6.23, 6.53 (meta-coupled doublets from ring protons). Mid-IR (cm^{-1}, CsI disks): ν(Mo═O), 917 (m), 907 (vs), 885 (vs); ν(Mo−O−Mo), 755 (m). Far-IR (cm^{-1}, CsI disks): 274 (m), 285 (m), 312 (m), 331 (s), 367 (m), 390 (m), 454 (m), 476 (m).

(Bu$_4$N)$_2$[Mo$_2$O$_5$(Cl$_4$-cat)(D^{t}BC)] (4). A THF solution (20 mL) of tetrachlorocatechol (0.10 g, 0.42 mmol) was slowly added to a CH_2Cl_2 solution (30 mL) of **1** (0.5 g, 0.42 mmol). The solution became pale green with time. When the addition was complete, the solution was filtered and 150 mL of diethyl ether was added to the filtrate. Upon standing overnight, 0.4 g of orange crystals formed, were isolated by filtration, and washed well with diethyl ether. The filtrate was pale blue/green. Anal. Calcd for $C_{52}H_{92}N_2O_9Cl_4Mo_2$ (MW = 1223.14): C, 51.06; H, 7.60; N, 2.29. Found: C, 51.04; H, 7.47; N, 2.34. Mass spectrum (FAB−, *m/e*): M$^-$ ([(Bu$_4$N)[Mo$_2$O$_5$(Cl$_4$-cat)(D^{t}BC)]$^-$) = 980; M$^-$ ([Mo$_2$O$_5$(Cl$_4$-cat)(D^{t}BC)]$^-$) = 738. Mass peaks corresponding to **1** or **3** are not present. Mid-IR (cm^{-1}, CsI disks): ν(C═C, catecholate), 1446 (vs); ν(C−O, catecholate), 1251 (m); ν(Mo═O), 926 (vs), 896 (vs); ν(Mo−O−Mo), 779 (m). Far-IR (cm^{-1}, CsI disks): 282 (vs), 292 (s), 328 (s), 332 (s), 347 (w), 366 (s), 379 (m), 400 (w), 449 (m), 464 (m), 480 (m), 483 (m).

(pyH)$_2$[[(py)(Cl$_4$-cat)MoO$_2$]$_2$(μ-O)] (5). This compound has been made previously through an unrelated synthesis.[19] An amount of (Bu$_4$N)$_2$[Mo$_2$O$_5$(Cl$_4$-cat)$_2$] (0.27 g, 0.22 mmol) was dissolved in 15 mL of CH_2Cl_2. An excess of pyridine (0.2 mL) was added, followed by 0.10 g (0.44 mmol) of pyH(PF$_6$). Addition of pyH$^+$ resulted in a dramatic color change from pale orange to deep red. After standing overnight, red crystals deposited which were isolated by filtration and washed thoroughly with diethyl ether. The spectroscopic characteristics for this compound are identical to those reported previously. Unfortunately, the crystals were twinned and verification of the unit cell parameters could not be achieved. Anal. Calcd for $C_{32}H_{26}N_4O_9Cl_8Mo_2$: C, 35.39; H, 2.42; N, 5.16. Found: C, 35.09; H, 2.26; N, 5.09. Mid-IR (cm^{-1}, CsI disks): ν(C═C, catecholate), 1449 (vs); ν(C−O, catecholate), 1261 (m); ν(Mo═O), 915 (vs), 887 (vs); ν(Mo−O−Mo), 755 (s); ν(pyridine), 3072 (w), 1604 (m), 695 (s). Far-IR (cm^{-1}, CsI disks): 283 (vs), 333 (w), 352 (w), 386 (s), 401(sh), 441 (w), 484 (w).

The same procedure using (Bu$_4$N)$_2$[Mo$_2$O$_5$(D^{t}BC)$_2$] as the starting complex resulted in a deep violet solution [585 nm (ϵ = 17 000 M^{-1} cm^{-1}), 344 nm (ϵ = 9000 M^{-1} cm^{-1})]. Separation of this product from Bu$_4$N(PF$_6$) proved difficult, and hence, no further characterization of the violet species was pursued.

(Bu$_4$N)$_2$[Mo$_2$O$_5$(M^{II}(TAD(O)$_2$))$_2$] (M = Ni, Co). An amount of M^{II}(TAD(OH)$_2$) (0.28 g, 0.62 mmol) was added to a CH_2Cl_2 solution (50 mL) of (Bu$_4$N)$_2$[Mo$_2$O$_7$] (0.24 g, 0.31 mmol). The solution was stirred for approximately 5 h, after which it was filtered. Diethyl ether (150 mL) was added to the filtrate, which after standing overnight yielded a dark oil. The solution was decanted, and the oil was redissolved in acetone or CH_2Cl_2 and layered carefully with 150 mL of diethyl ether. Crystals were subsequently obtained in 80% yield.

(A) M = Co (6). Solutions of this complex are deep red. Anal. Calcd for $C_{80}H_{112}N_{10}O_9Co_2Mo_2 \cdot {}^1/_2CH_2Cl_2$: C, 56.53; H, 6.67; N, 8.19. Found: C, 56.45; H, 6.12; N, 8.06. Mid-IR (cm^{-1}, CsI disks): ν(C═N), 1520 (vs); ν(C═C), 1475 (vs); ν(C−O), 1286 (s); ν(Mo═O), 929 (s), 901 (s); ν(Mo−O−Mo), 790 (m). Far-IR (cm^{-1}, CsI disks): 274 (m), 279 (m), 313 (sh), 320 (sh), 325 (m), 348 (w), 367 (w), 385 (vs), 418 (m), 445 (w), 460 (m).

(B) M = Ni (7). Solutions of this complex are deep green. Anal. Calcd for $C_{80}H_{112}N_{10}O_9Ni_2Mo_2$: C, 57.63; H, 6.78; N, 8.40. Found: C, 57.53; H, 6.83; N, 8.39. Mid-IR (cm^{-1}, CsI disks): ν(C═N), 1520 (vs); ν(C═C), 1475 (vs); ν(C−O), 1286 (s); ν(Mo═O), 929 (s), 901 (s); ν(Mo−O−Mo), 790 (m). Far-IR (cm^{-1}, CsI disks): 274 (m), 279 (m), 313(sh), 320(sh), 325 (m), 348 (w), 367 (w), 385 (vs), 418 (m), 445 (w), 460 (m). Single crystals of this complex were the subject of an X-ray structure determination.

(Bu$_4$N)$_2$[Mo$_2$O$_5$(H$_2$(R$_2$R′$_2$SALPHEN(O)$_2$))$_2$ (R = R′ = H; R = R′ = *tert*-Butyl; R = EtO, R′ = H). These complexes were synthesized in a manner similar to that described for **1**−**3**, except where indicated. Yields of orange powder in all cases were in excess of 80%.

R = R′ = H (8). Reagent quantities: 0.59 g (0.75 mmol) of (Bu$_4$N)$_2$[Mo$_2$O$_7$], 0.53 g (1.5 mmol) of SALPHEN catechol. After the solution was stirred for 5 h, the solvent was removed under vacuum. The residue was recrystallized from THF/diethyl ether. An oily orange product was obtained, which was obtained as an orange powder after thorough washing with diethyl ether. Anal. Calcd for $C_{72}H_{100}N_6O_{13}Mo_2$ (MW = 1449.66): C, 59.65; H, 6.97; N, 5.80. Found: C, 60.00; H, 7.20; N, 6.32. Mass spectrum (FAB−, *m/e*): M$^-$ ([(Bu$_4$N)[Mo$_2$O$_5$(H$_2$SALPHEN(O)$_2$)$_2$]$^-$) = 1207; M$^-$ ([Mo$_2$O$_5$(H$_2$SALPHEN(O)$_2$)$_2$]$^-$) = 966. Mid-IR (cm^{-1}, CsI disks): ν(C═N), 1581 (s); ν(C═C), 1488 (vs); ν(C−O), 1278 (v); ν(Mo═O), 933 (sh), 922 (s), 901 (vs); ν(Mo−O−Mo), 760 (m). Far-IR (cm^{-1}, CsI disks): 312 (vs), 322 (sh), 374 (sh), 383 (s), 430 (m), 442 (w), 471 (w).

R = R′= *tert*-Butyl (9). Reagent quantities: 0.24 g (0.31 mmol) of (Bu$_4$N)$_2$[Mo$_2$O$_7$], 0.40 g (0.62 mmol) of SALPHEN catechol. After the solution was stirred for 5 h, the solvent was removed under vacuum.

(19) Blatchford, T. P.; Chisolm, M. H.; Huffman, J. C. *Inorg. Chem.* **1988**, *27*, 2059.

The residue was recrystallized from toluene/hexanes. Anal. Calcd for $C_{104}H_{164}N_6O_{13}Mo_2$ (MW = 1898.62): C, 65.79; H, 8.72; N, 4.43. Found: C, 64.81; H, 8.80; N, 4.67. Mass spectrum (FAB−, *m/e*): M^- ($[(Bu_4N)[Mo_2O_5(H_2(^tBu_4SALPHEN(O)_2)_2]^-)$ = 1657; M^- ($[Mo_2O_5(H_2(^tBu_4SALPHEN(O)_2)_2]^-)$ = 1415. Mid-IR (cm^{-1}, CsI disks): ν(C═N), 1592 (m); ν(C═C), 1481 (vs); ν(C−O), 1276 (s); ν(Mo═O), 933 (s), 921 (s), 901 (vs): ν(Mo−O−Mo), 760 (w). Far-IR (cm^{-1}, CsI disks): 313 (vs), 329 (sh), 374 (m), 387 (m), 410 (w), 497 (vs).

R = EtO, R′ = H (10). To a slurry of $[H_2(EtO_2H_2SALPHEN(OH)_2)]$·pyHBr (1.80 g, 3.0 mmol) in 50 mL of CH_2Cl_2 was added 0.42 mL of Et_3N (3.0 mmol) in order to neutralize the pyHBr and solubilize the ligand. $(Bu_4N)_2[Mo_2O_7]$ (1.20 g, 1.5 mmol) was then added and the orange solution stirred for 3 h. The solvent was removed *in vacuo*, the residue was redissolved in THF and filtered to remove a quantitative yield of Et_3NHBr, and diethyl ether (150 mL) was added to the filtrate to induce precipitation of the product. Anal. Calcd for $C_{80}H_{116}N_6O_{17}Mo_2$ (MW = 1625.90): C, 59.09; H, 7.21; N, 5.17. Found: C, 58.40; H, 7.21; N, 5.49. Mass spectrum (FAB−, *m/e*): M^- ($[(Bu_4N)[Mo_2O_5(H_2(EtO_2H_2SALPHEN(O)_2))_2]^-$) = 1383; M^- ($[Mo_2O_5(H_2(EtO_2H_2SALPHEN(O)_2))_2]^-$) = 1141. Mid-IR ($cm^{-1}$, CsI disks): ν(C═N), 1607 (s); ν(C═C), 1488 (vs); ν(C−O), 1278 (vs); ν(Mo═O), 934 (sh), 920 (vs), 902 (vs); ν(Mo−O−Mo), 750 (m). Far-IR (cm^{-1}, CsI disks), 308 (vs), 315 (sh), 330 (sh), 370 (w), 385 (m), 470 (m), 491 (s).

$(Bu_4N)_2[Mo_2O_5(M^{II}(R_2R'_2SALPHEN(O)_2))_2]$ (M = Mn (R = EtO, R′ = H; 11), Fe (R = R′ = *tert*-Butyl, 12; R = EtO, R′ = H; 13), Co (R = R′= *tert*-Butyl, 14; R = EtO, R′ = H; 15), Ni (R = R′ = *tert*-Butyl, 16; R = EtO, R′ = H; 17), Cu (R = R′ = *tert*-Butyl, 18; R = EtO, R′ = H; 19)). A general procedure was followed, with exceptions noted. An amount of $(Bu_4N)_2[Mo_2O_5(H_2(R_2R'_2SALPHEN(O)_2))_2]$ was dissolved in 30 mL of acetone. A methanolic solution (40 mL) of $M^{II}(OAc)_2$·nH_2O (2 equiv; M = Mn, Co, Ni, n = 4; M = Cu, n = 2) was added dropwise with stirring. The solution became deep orange/red. After about 1 h of stirring, the solution was filtered and the solvent removed under vacuum. The residue was redissolved in THF/CH_2Cl_2 (10:1, for R = R′ = H and R = EtO, R′ = H) or toluene (R = R′ = ^{t}Bu), filtered, and precipitated using diethyl ether or hexanes, respectively. After overnight standing, a crop of orange/red microcrystalline material was obtained in near-quantitative yield. Reagent quantities, deviations from this general procedure, and analytical and spectroscopic data for complexes **11**−**18** are provided in the Supporting Information.

R = EtO, R′ = H; M = Cu (19). Reagent quantities: 0.61 g (0.37 mmol) of **10**, 0.15 g (0.75 mmol) of $Cu(OAc)_2$·$2H_2O$. Yield: 0.55 g. Anal. Calcd for $C_{80}H_{112}N_6O_{17}Cu_2Mo_2$: C, 54.94; H, 6.47; N, 4.81. Found: C, 54.62; H, 6.56; N, 5.08. Mid-IR (cm^{-1}, CsI disks): ν(C═N), 1601 (vs); ν(C═C), 1492 (vs); ν(C−O), 1290 (v); ν(Mo═O), 928 (vs), 905 (vs); ν(Mo−O−Mo), 740 (m). Far-IR (cm^{-1}, CsI disks): 275 (m), 335 (vs), 383 (m), 392 (m). Crystals suitable for an X-ray diffraction study were obtained by diffusion of diethyl ether into a THF solution of the complex.

$(Bu_4N)_2[Mo_2O_5(D^tBC)(M(^tBu_4SALPHEN(O)_2)]$ (M = $(H^+)_2$, Co^{II}, Ni^{II}). $(Bu_4N)_2[Mo_2O_5(D^tBC)_2]$ (0.6 g, 0.5 mmol) was dissolved in 40 mL of CH_2Cl_2. A CH_2Cl_2 solution (40 mL) of $M(^tBu_4SALPHEN(OH)_2)$ (0.50 mmol) was added dropwise over approximately 1 h to a stirring solution of the complex. After the addition was complete, the solution volume was decreasd to 30 mL and diethyl ether was added to induce precipitation. After standing for 2 days, the product was obtained as a powder by filtration. The filtrate was pale green. The product was recrystallized once from THF/diethyl ether and obtained pure in approximately 70% yield.

M = $(H^+)_2$ (20). Anal. Calcd for $C_{82}H_{138}N_4O_{11}Mo_2$: C, 63.61; H, 9.00; N, 3.62. Found: C, 63.27; H, 8.91; N, 3.59. NMR (δ, ppm): 6.21, 6.70 (*meta*-coupled doublets) from D^tBC; 6.40 (singlet, catecholate protons), 7.28, 7.37 (*meta*-coupled doublets from protons on phenol ring), 8.53 (singlet, N═C*H*) from SALPHEN. Mid-IR (cm^{-1}, CsI disks): ν(C═N), 1592 (m); ν(C═C), 1486 (vs), ν(C−O), 1270 (s); ν(Mo═O), 919 (vs), 892 (vs). Far-IR (cm^{-1}, CsI disks): 301 (s), 314 (s), 327 (m), 368 (w), 380 (w), 389 (w), 410 (w), 453 (w), 478 (m), 496 (s).

M = Co^{II} (21). Anal. Calcd for $C_{82}H_{136}N_4O_{11}CoMo_2$ (MW = 1605.03): C, 61.36; H, 8.56; N, 3.49. Found: C, 62.16; H, 8.59; N, 3.91. Mass spectrum (ES−, *m/e*): 1363.0 (M − Bu_4N^+ = 1362.5). Mid-IR (cm^{-1}, CsI disks): ν(C═N), 1592 (m); ν(C═C), 1486 (vs); ν(C−O), 1268 (s); ν(Mo═O), 922 (vs), 916 (vs), 892 (vs). Far-IR (cm^{-1}, CsI disks): 327 (m), 395 (w), 451 (w), 495 (s).

(C) M = Ni^{II} (22). Anal. Calcd for $C_{82}H_{136}N_4O_{11}NiMo_2$ (MW = 1604.80): C, 61.37; H, 8.56; N, 3.49. Found: C, 61.54; H, 8.74; N, 3.49. Mass spectrum (ES−, *m/e*): 1362.3 (M − Bu_4N^+ = 1362.3). Mid-IR (cm^{-1}, CsI disks): ν(C═N), 1592 (m); ν(C═C), 1486 (vs); ν(C−O), 1270 (s); ν(Mo═O), 923 (vs), 892 (vs). Far-IR (cm^{-1}, CsI disks): 302 (w), 313 (w), 327 (s), 366 (m), 398 (s), 414 (w), 452 (m), 495 (vs).

$(Bu_4N)_2[Mo_2O_5(D^tBC)(Fe(^tBu_4SALPHEN(O)_2)]$ (23). A procedure similar to that employed in the synthesis of **12** was used. Reagent quantities: 0.53 g of **20** (0.34 mmol), 0.06 g of $Fe(OAc)_2$ (0.34 mmol). After overnight standing, filtration yielded 0.5 g of a red/brown powder. Anal. Calcd for $C_{82}H_{136}N_4O_{11}FeMo_2$: C, 61.48; H, 8.57; N, 3.50. Found: C, 61.22; H, 8.22; N, 3.61. Mid-IR (cm^{-1}, CsI disks): ν(C═N), 1598 (m); ν(C═C), 1485 (vs); ν(C−O), 1281 (s); ν(Mo═O), 926 (s), 910 (s), 895 (s). Far-IR (cm^{-1}, CsI disks): 327 (s), 350 (m), 370 (m), 482 (s).

$(Bu_4N)_2[Mo_2O_5(D^tBC)(Cu(^tBu_4SALPHEN(O)_2))]$ (24). **20** (0.64 g, 0.41 mmol) was dissolved in 40 mL of acetone. $Cu(OAc)_2$·$2H_2O$ (0.09 g, 0.45 mmol) was dissolved in 40 mL of MeOH, and the solution was added dropwise with stirring to the solution of **20**. The solution was stirred for a total of 3 h, during which it assumed the characteristic orange/red color of the metalated derivatives. The solution was filtered, and the volatiles were removed from the filtrate under vacuum. The residue was recrystallized from THF/diethyl ether. Upon standing overnight, a red powder deposited and was isolated (yield = 0.5 g). Anal. Calcd for $C_{82}H_{136}N_4O_{11}CuMo_2$ (MW = 1609.65): C, 61.18; H, 8.53; N, 3.48. Found: C, 60.72; H, 8.32; N, 3.44. Mass spectrum (ES−, *m/e*): 1367.1 (M − Bu_4N^+ = 1367.1). Mid-IR (cm^{-1}, CsI disks): ν(C═N), 1598 (s); ν(C═C), 1485 (vs); ν(C−O), 1278 (s); ν(Mo═O), 923 (vs), 913 (vs), 891 (vs). Far-IR (cm^{-1}, CsI disks): 328 (s), 352 (m), 495 (vs).

$[Mo_2O_5(M(^tBu_4SALPHENSQ(O)_2))_2]$ (M = $(H^+)_2$ (25), Co^{II} (26), or Ni^{II} (27)). The corresponding bis(SALPHEN-catecholate) complex was dissolved in 50 mL of CH_3CN. Two equivalents of $FcPF_6$ were added in one portion, and the solution was stirred for 2 h. The solution was filtered, and the filtrate was taken to dryness. The resulting residue was taken up in diethyl ether (M = H_2) or toluene (M = Co^{II}, Ni^{II}) and filtered to remove a quantitative yield of $Bu_4N(PF_6)$. The filtrate was again taken to dryness. As the resulting residue was at least partially soluble in all organic solvents employed, the ferrocene was removed by sublimation using a coldfinger while gently warming the reaction flask under vacuum. The remaining residue was collected and found to be analytically pure. Reagent quantities and analytical and spectroscopic data for complexes **26** and **27** are provided in the Supporting Information.

M = $(H^+)_2$ (25). Reagent quantities: 0.6 g of **9** (0.32 mmol), 0.21 g of $FcPF_6$ (0.64 mmol). Anal. Calcd for $C_{72}H_{92}N_4O_{13}Mo_2$ (MW = 1413.56): C, 61.17; H, 6.57; N, 3.96. Found: C, 61.16; H, 6.73; N, 3.97. Mass spectrum (ES−, *m/e*): 1413.1 (M − H^+ = 1412.6). Mid-IR (cm^{-1}, CsI disks): ν(C═N), 1592 (m); ν(C═C), 1481 (vs); ν(C−O), 1276 (s); ν(Mo═O), 933 (s), 921 (s), 901 (vs); ν(Mo−O−Mo), 760 (m). Far-IR (cm^{-1}, CsI disks): 313 (s), 329 (sh), 374 (m), 387 (m), 410 (w), 497 (vs).

$[Mo_2O_5(M(EtO_2H_2SALPHENSQ(O)_2))_2]$ (M = $(H^+)_2$ (28), Co^{II} (29), Ni^{II} (30)). Two equivalents of $Fc(PF_6)$ were added to an CH_3CN solution (30 mL) of the corresponding bis(catecholate) complex. Precipitation of a red/brown solid occurred immediately. The reaction was stirred for 1 h, after which it was filtered to obtain the product. The color of the filtrate was the characteristic orange of ferrocene. The solid was washed with small portions of ethanol and diethyl ether and dried under vacuum. Yields were essentially quantitative. Reagent quantities and analytical and spectroscopic data for complexes **29** and **30** are provided in the Supporting Information.

M = $(H^+)_2$ (28). Reagent quantities: **10**, 0.50 g (0.31 mmol); $Fc(PF_6)$, 0.20 g (0.60 mmol). Anal. Calcd for $C_{48}H_{44}N_4O_{17}Mo_2$·$CH_3CN$: C, 50.81; H, 4.02; N, 5.95. Found: C, 50.69; H, 4.12; N, 6.28.

Mid-IR (cm^{-1}, CsI disks): ν(C═N), 1609 (m); ν(C═C), 1487 (vs); ν(C−O), 1273 (vs); ν(Mo═O), 935 (s), 906 (s); ν(Mo−O−Mo), 739 (m); ν(CN, CH_3CN), 2249 (w). Far-IR (cm^{-1}, CsI disks): 275 (m), 335 (vs), 383 (m), 392 (m).

$(Et_4N)_2[[(x)(Ni(EtO_2H_2SALPHENSQ)(O)_2)MoO_2]_2)(\mu$-O)] (X = SCN^-, CN^-). Two equivalents of $Et_4N(X)$ were added to a slurry of **30** in 1:1 (v/v) CH_3CN/CH_3NO_2 (50 mL). The complex dissolved within the first hour of stirring, after which the solution was filtered and layered with diethyl ether. After overnight standing, a near-quantitative yield of red microcrystalline material was obtained by filtration.

$(Et_4N)_2[[(SCN)(Ni(EtO_2H_2SALPHENSQ(O)_2))MoO_2]_2(\mu$-O)] (31). Reagent quantities: **30**, 0.40 g (0.32 mmol); $Et_4N(SCN)$, 0.12 g (0.64 mmol). Anal. Calcd for $C_{66}H_{80}N_8O_{17}S_2Ni_2Mo_2$: C, 48.60; H, 4.95; N, 6.87. Found: C, 48.70; H, 4.95; N, 6.64. Mid-IR (cm^{-1}, CsI disks): ν(C═N), 1603 (s); ν(C═C), 1490 (vs); ν(C−O), 1294 (vs); ν(Mo═O), 933 (s), 905 (s); ν(Mo−O−Mo), 740 (m); ν(SCN), 2085 (m). Far-IR (cm^{-1}, CsI disks): 277 (vs), 298 (sh), 327 (m), 361 (w), 385 (s), 405 (s), 437 (m), 472 (w).

$(Et_4N)_2[[(CN)(Ni(EtO_2H_2SALPHENSQ(O)_2))MoO_2]_2(\mu$-O)]·$2CH_3CN$ (32). Reagent quantities: **30**, 0.40 g (0.32 mmol); $Et_4N(CN)$, 0.10 g (0.64 mmol). Anal. Calcd for $C_{70}H_{86}N_{10}O_{17}Ni_2Mo_2$: C, 50.98; H, 5.27; N, 8.50. Found: C, 50.95; H, 5.39; N, 8.54. Mid-IR (cm^{-1}, CsI disks): ν(C═N), 1603 (s); ν(C═C), 1490 (vs); ν(C−O), 1294 (vs); ν(Mo═O), 933 (s), 905 (s); ν(Mo−O−Mo), 740 (m); ν(CN), 2170 (w), 2118 (w); ν(CN, CH_3CN), 2249 (w). Far-IR (cm^{-1}, CsI disks): 277 (vs), 298 (sh), 327 (m), 361 (w), 385 (s), 405 (s), 437 (m), 472 (w).

$[Mo_2O_5(D^tBSQ)(H_2(^tBu_4SALPHENSQ(O)_2))]$ (33). 20 (0.91 g, 0.59 mmol) was dissolved in 50 mL of CH_3CN. $FcPF_6$ (0.39 g, 1.2 mmol) was added in small portions. The solution immediately becomes the characteristic yellow/green color. The reaction was stirred for 1 h, after which the solvent was removed under vacuum. The resulting residue was taken up in toluene and filtered to remove a quantitative amount of $Bu_4N(PF_6)$, and hexanes (150 mL) was added to the filtrate to induce precipitation. After standing for 2 days, 0.4 g (65% yield) of brown powder was obtained by filtration. Anal. Calcd for $C_{50}H_{66}N_2O_{11}Mo_2·CH_3CN$: C, 56.56; H, 6.31; N, 3.81. Found: C, 56.23; H, 6.64; N, 3.92. Electronic spectrum [nm (ϵ, $M^{-1}\,cm^{-1}$), CH_3CN solution]: 366 (23 000), 316 (sh), 273 (sh), 273 (sh), 230 (sh). Mid-IR (cm^{-1}, CsI disks): ν(C═N), 1595 (m); ν(C═C), 1483 (vs); ν(C−O), 1300 (m); ν(Mo═O), 930 (s), 905 (s), ν(CN, CH_3CN), 2249 (w).

$(Bu_4N)_2[Mo_2O_5[(Fe(EtO_2H_2SALPHEN(O)_2))_2(\mu$-O)]]·$^1/_2CH_2Cl_2$ (34). $(Bu_4N)_2[Mo_2O_5(Fe(EtO_2H_2SALPHEN(O)_2))_2]$ (0.64 g, 0.35 mmol) was dissolved in 40 mL of CH_3CN. Dry O_2 was bubbled through this solution at ambient temperature for approximately 1 h. The solution was then removed under vacuum, and the residue was recrystallized from CH_2Cl_2/diethyl ether. The product is only sparingly soluble in THF, unlike the starting complex **13**. Upon standing overnight, 0.6 g of red/brown crystals formed and were isolated by filtration. Yield: 95%. Anal. Calcd for $C_{80.5}H_{113}N_6O_{18}ClFe_2Mo_2$: C, 53.95; H, 6.37; N, 4.69. Found: C, 53.85; H, 6.28; N, 4.96. Mid-IR (cm^{-1}, CsI disks): ν(C═N), 1599 (vs); ν(C═C), 1494 (vs); ν(C−O), 1288 (vs); ν(Mo═O), 940 (s), 926 (s), 907 (m); ν(Mo−O−Mo), 738 (m); ν(Fe−O−Fe), 595 (m). Far-IR (cm^{-1}, CsI disks): 296 (w), 303 (w), 316 (sh), 327 (s), 332 (sh), 384 (m), 492 (vs).

$(Bu_4N)_2[Mo_2O_5[(Fe(EtO_2H_2SALPHEN(O)_2))_2(\mu$-S)]]·$CH_2Cl_2$ (35). $(Bu_4N)_2[Mo_2O_5(Fe(EtO_2H_2SALPHEN(O)_2))_2]$ (0.46 g, 0.25 mmol) was dissolved in 40 mL of CH_2Cl_2. A solution of benzyl trisulfide was pepared in 40 mL of acetone, which was added dropwise to the complex solution over 1 h. The reaction was stirred for an additional 1 h, after which it was filtered. Diethyl ether was added to the filtrate and allowed to diffuse slowly. Upon standing overnight, 0.3 g (65%) of red/brown microcrystalline solid formed and was isolated by filtration. Anal. Calcd for $C_{81}H_{114}N_6O_{17}Cl_2SFe_2Mo_2$: C, 52.58; H, 6.22; N, 4.54. Found: C, 52.44; H, 5.89; N, 4.89. Mid-IR (cm^{-1}, CsI disks): ν(C═N), 1598 (vs); ν(C═C), 1486 (vs); ν(C−O), 1284 (vs); ν(Mo═O), 940 (s), 926 (s), 907 (m); ν(Mo−O−Mo), 740 (m). Far-IR (cm^{-1}, CsI disks): 270 (w), 291 (w), 303 (w), 328 (sh), 335 (s), 384 (w), 436 (m, possibly from Fe−S−Fe), 494 (vs).

Table 1. Crystal and Structure Refinement Data for $(Bu_4N)_2[Mo_2O_5(Ni(TAD(O)_2))_2]$ (**7**) and $(Bu_4N)_2[Mo_2O_5(Cu(EtO_2H_2SALPHEN(O)_2))_2]$ (**19**)

	7	**19**
empirical formula	$C_{80}H_{112}N_{10}O_9Ni_2Mo_2$	$C_{80}H_{112}N_6O_{17}Cu_2Mo_2$
formula mass	1667.10	1748.72
cryst system	triclinic	monoclinic
space group	$P\bar{1}$	$P2_1/c$
unit cell dimens	a = 12.324(3) Å b = 17.740(4) Å c = 20.920(4) Å α = 108.79(3)° β = 98.20(3)° γ = 103.12(3)°	a = 20.821(4) Å b = 23.133(5) Å c = 20.056(4) Å β = 117.71(3)°
V, Z	4099.5(14) $Å^3$, 2	8552(3) $Å^3$, 4
D(calcd)	1.351 g/mL	1.358 g/mL
abs coeff	0.811 mm^{-1}	0.843 mm^{-1}
F(000)	1748	3648
ω-range for data collcn	3.0−45.0°	3.0−40.0°
limiting indices	$+h,\pm k,\pm l$	$+h,+k,\pm l$
reflcns collcd	11300	8322
indepdt reflcns	10699 [R(int) = 0.1332]	8018 [R(int) = 0.0511]
data/restraints/params	10686/0/826	8018/0/558
GOF on F^2	1.528	1.040
final R indices [$I > 2\sigma(I)$]	$R1$[a] = 0.0967, w$R2$[b] = 0.2335	$R1$ = 0.0995, w$R2$ = 0.2058
largest diff peak and hole	1.726 and −1.339 e·$Å^{-3}$	0.757 and −0.591 e·$Å^{-3}$

[a] $R1 = \sum||F_o| - |F_c||/\sum|F_o|$. [b] $wR2 = [\sum[w(F_o^2 - F_c^2)]^2/[\sum[w(F_o^2)^2]]^{1/2}$.

Crystallography. Collection and Reduction of X-ray Data. Specific information is provided in Table 1. Single crystals of $(Bu_4N)_2[Mo_2O_5(Ni(TAD(OH)_2))_2]$, **7**, were grown by diffusion of diethyl ether into an acetone solution of the complex. Single crystals of $(Bu_4N)_2[Mo_2O_5(Cu(EtO_2SALPHEN(OH)_2))_2]$, **19**, were grown by diffusion of diethyl ether into a dichloromethane solution of the complex. Crystals were mounted with Apiezon grease in a glass capillary (Charles Supper Co.) under an Ar atmosphere, and the capillary was then flame sealed. Data collection was carried out at ambient temperature on a Nicolet P3F four-circle, computer-controlled diffractometer equipped with a graphite monochromator. The final orientation matrix and unit cell parameters were determined from 20 machine-centered reflections. Monitoring of the three standard reflections every 97 measurements indicated no decay of the crystal over the period of data collection. The raw data were reduced to net intensities, estimated standard deviations were calculated on the basis of counting statistics, and equivalent reflections were averaged. Computer programs used were from the SHELXTL structure determination package (Nicolet XRD Corp., Madison, WI).

Structure Solution and Refinement. The direct methods routine of SHELXTL version 5.06 (1994) was employed. Trial positions of the Mo and Ni (Cu) atoms were taken from the *E*-map derived from the phase set with the highest combined figure of merit. The positions of the remaining non-hydrogen atoms were determined by subsequent difference Fourier maps. The structures were refined by the full-matrix least-squares method. The asymmetric units consist of a complete anion and two tetrabutylammonium (Bu_4N^+) cations. For **7**, all of the atoms were assigned anisotropic temperature factors except for the methyl groups on the macrocycles and the carbon atoms of the disordered cations. For **19**, due to limited data obtained from the best available poorly diffracting crystal, only the metal atoms and the atoms bonded to them were assigned anisotropic temperature factors. The H atoms were assigned fixed positions (C−H bond length of 0.96 Å) except for the carbon atoms of the disordered cations, where hydrogen contributions were not included.

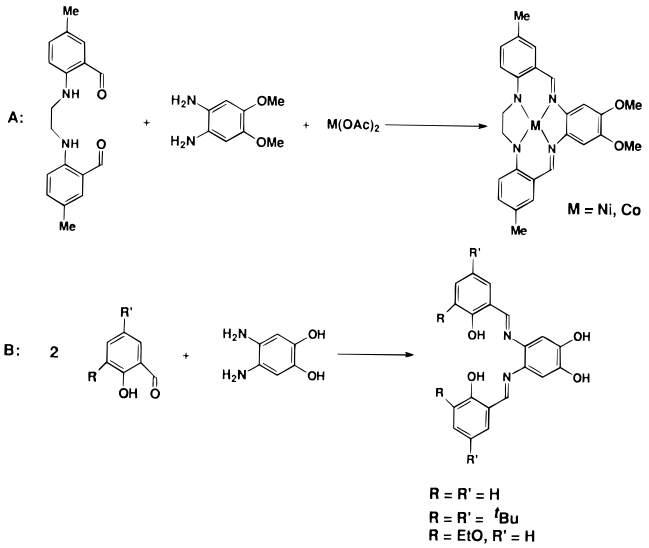

Figure 2. Synthesis of the ligands (A) $M^{II}(TAD(OMe)_2)$ and (B) $H_2(R_2R'_2SALPHEN(OH)_2)$.

Results and Discussion

The synthesis of the $M^{II}(TAD(OH)_2)$ (M = Ni, Co) macrocyclic complexes has been reported previously.[1] These complexes form from Schiff-base condensations between the appropriate dialdehyde and 4,5-diaminoveratrole using a metal(II) ion as a templating agent (Figure 2A). The catechol group is "deprotected" through subsequent removal of the methyl groups. Currently, only the Ni^{II} and Co^{II} macrocycles can be synthesized conveniently by this route. After the macrocyclic-catechol work, the synthesis of catechol-functionalized SALPHEN complexes was developed and their chemistry is being pursued in our laboratory.[2] The metal-free SALPHEN-catechol multifunctional ligands are readily synthesized from 4,5-diaminocatechol and 2 equiv of the appropriate salicylaldehyde (Figure 2B) and can be metalated in a subsequent step. The SALPHEN-catechol ligands represent a convenient alternative to the macrocyclic catechols as they are easier to synthesize with a wide variety of di- and trivalent metal ions.[20] The flexibility in the variation of substituents that can be introduced to the phenyl rings also allows for diversity in properties such as steric bulk and solubility.

The synthesis of cofacially-oriented porphyrin complexes, with rigid aromatic or flexible amide bridging units, and the reactivity of these molecules have been the subject of extensive studies by Collman[4] and Chang.[5] The properties of these molecules, including their utility in the activation of O_2,[5c,8,9] have been reported. The synthesis of catechol-functionalized macrocyclic and SALPHEN complexes and the unique characteristics of the cofacial porphyrin "dimers" prompted us to explore the use of the former as ligands in the design of new supermolecular assemblies with cofacially-oriented, planar, metal-containing subunits.

The synthesis of the $[Mo_2O_5]^{2+}$-bridged, cofacially-oriented macrocyclic and SALPHEN complexes reported here was inspired by known complexes that contain $[Mo_2O_5]^{2+}$ bridges between simple catecholate or semiquinone ligands. These include the $(Bu_4N)_2[Mo_2O_5(3,5\text{-}R_2\text{catecholate})_2]$ (R = H,[13] ^{t}Bu[14]) and [[(9,10-phenanthrenesemiquinone)MoO_2]$_2$(μ-O)][15] complexes.

The synthesis of the $(Bu_4N)_2[Mo_2O_5(D^tBC)_2]$ (**1**) complex previously described involves the reaction of $MoO_2(acac)_2$ with 2 equiv of 3,5-di-*tert*-butylcatechol to afford the dimer [MoO-(D^tBC)$_2$]$_2$.[14b,c,21] Reaction of this dimer with OH^- yielded **1** (Figure 3A). The second step in this approach is rather vaguely defined with regard to the number of equivalents of OH^- required and whether the synthesis requires O_2 as a "catalyst". We sought a new synthetic route to these complexes using $(Bu_4N)_2[(MoO_3)_2(\mu\text{-O})]$, which is obtained in large quantities from a simple 2-step synthesis.[18] The reactivity of one of the Mo=O groups in each of the two MoO_3 units in $(Bu_4N)_2$-$[(MoO_3)_2(\mu\text{-O})]$ has its origin in the "spectator" Mo=O-group effect previously described[22] and associated with the exceptional stability of the quasi-square pyramidal Mo(VI) ions in the final product. The anticipated reaction of $(Bu_4N)_2[Mo_2O_7]$ with 2 equiv of 3,5-di-*tert*-butylcatechol took place to yield **1** in 90% yield (Figure 3B). Spectroscopic properties of **1** obtained from this latter convenient synthesis were consistent with those reported previously.[14b,c] The reaction is quite general and proceeds with carboxylic acids (vide infra) and also with the macrocyclic- and SALPHEN-catechol ligands and metal complexes thereof. The use of $(Bu_4N)_2[(MoO_3)_2(\mu\text{-O})]$ as a reagent in the low-yield synthesis of $(Bu_4N)_2[Mo_4O_{10}(C_6H_2O_4)_2]$ from 2,5-dihydroxy-1,4-benzoquinone has been described previously.[23] This molecule contains cofacial semiquinones which are bridged by two $[Mo_2O_5]^{2+}$ units.

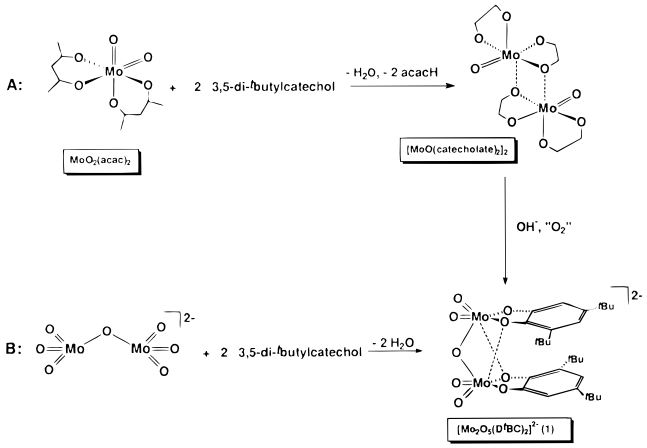

Figure 3. Synthesis of **1** from (A) a previously published procedure[14b,c] and (B) the new synthesis from $[Mo_2O_7]^{2-}$ as described in the text.

A survey of the literature provides a number of examples of molecules with the general formulation $[((L)(L')MoO_2)_2(\mu\text{-O})]^{n-}$ (L = L′ = 9,10-phenanthrenesemiquinone,[15] *N*-(2-mercaptoethyl)-*N*′,*N*′-dimethylethylenediamine,[24] or *N*,*N*-bis(2-pyridylmethyl)-2-mercaptoethylamine,[24] n = 0; L = phenanthroline, L′ = NCS^-,[25] n = 0; L = L′ = catecholate,[13,14] nitrilotriacetate (NTA),[26] or citrate;[27] n = 2; L = tetrachlorocatecholate, L′ = pyridine[19] or L = oxalate, L′ = H_2O,[28] n = 2). Except for $(pyH)_2$[[(py)(Cl_4-cat)MoO_2]$_2$(μ-O)], these complexes are generally formed from the reaction of MoO_3 or MoO_4^{2-} and the

(20) Rosa, D. T.; Coucouvanis, D. To be submitted separately.

(21) Buchanan, R. M.; Pierpont, C. G. *Inorg. Chem.* **1979**, *18*, 1616.
(22) (a) Rappe, A. K.; Goddard, W. A., III. *J. Am. Chem. Soc.* **1982**, *104*, 448. (b) Rappe, A. K.; Goddard, W. A., III *J. Am. Chem. Soc.* **1980**, *102*, 5115.
(23) Liu, S.; Shaikh, S. N.; Zubieta, J. *Inorg. Chem.* **1989**, *28*, 723.
(24) Marabella, C. P.; Enemark, J. H.; Miller, K. F.; Bruce, A. E.; Pariyadath, N.; Corbin, J. L.; Stiefel, E. I. *Inorg. Chem.* **1983**, *22*, 3456.
(25) Viossat, B.; Rodier, N. *Acta Crystallogr., Sect. B* **1981**, *B37*, 56.
(26) Knobler, C.; Penfold, B. R.; Robinson, W. T.; Wilkins, C. J.; Yong, S. H. *J. Chem. Soc., Dalton Trans.* **1980**, 248.
(27) Zhou, Z.-H.; Wan, H.-L.; Tsai, K.-R. *Polyhedron* **1997**, *16*, 75.
(28) Cotton, F. A.; Morehouse, S. M.; Wood, J. S. *Inorg. Chem.* **1964**, *3*, 1603.

conjugate acid of the ligand in aqueous medium or from $MoO_2(acac)_2$ and the conjugate acid in organic solvents. In both cases, the pathway to product formation is not entirely clear, with the formation of the oxo bridge most likely resulting from deprotonation of nascent H_2O that binds to the Mo atom.

The synthesis of **1**−**3** from the appropriate catechol and $[(MoO_3)_2(\mu\text{-}O)]^{2-}$ is straightforward and involves removal of one oxo group per Mo following protonation by the acidic ligand. It appeared likely that this synthetic strategy may be of general utility, providing a direct route to a number of molecules with the $[(MoO_2)_2(\mu\text{-}O)]^{2+}$ core, including those obtained previously by other synthetic procedures. The reaction of $[(MoO_3)_2(\mu\text{-}O)]^{2-}$ with 2 equiv of (methylimino)diacetic acid (MIDA) gave $[((MIDA)MoO_2)_2(\mu\text{-}O)]^{2-}$ in good yield. This is similar to the $[((NTA)MoO_2)_2(\mu\text{-}O)]^{2-}$ complex synthesized previously from the reaction of nitrilotriacetic acid (NTA), hydroxide, and MoO_3 in H_2O[26] (MIDA and NTA differ only in the nature of the nonbonding "arm" of the ligand). This result supports the expectation that the $[(MoO_3)_2(\mu\text{-}O)]^{2-}$ dianion may be of general synthetic utility.

Synthesis of Supermolecular Bis(catecholato) Complexes. The successful synthesis of **1** using $[Mo_2O_7]^{2-}$ provided a convenient route to the synthesis of derivatives that incorporate metalated macrocyclic- and SALPHEN-catecholates bridged by $[Mo_2O_5]^{2+}$ in place of the simple catecholates. The reaction between $(Bu_4N)_2[(MoO_3)_2(\mu\text{-}O)]$ and 2 equiv of $M^{II}(TAD(OH)_2)$ (M = Ni, Co) or the various metal-free SALPHEN-catechol ligands in organic solvents (CH_2Cl_2 or toluene) at ambient temperature offers a straightforward route to the supermolecular cofacial bis(catecholate) complexes $(Bu_4N)_2[Mo_2O_5(M^{II}(TAD\text{-}(O)_2))_2]$ (M = Co (**6**) or Ni (**7**)) and $(Bu_4N)_2[Mo_2O_5(H_2(R_2R'_2\text{-}SALPHEN(O)_2))_2]$ (R = R′ = H (**8**), R = R′= *tert*-butyl (**9**), or R = EtO, R′ = H (**10**)) (Figure 4). Complex **7** has been characterized by an X-ray diffraction study and provides confirmation that the product is structurally similar to that obtained by the reaction of $(Bu_4N)_2[(MoO_3)_2(\mu\text{-}O)]$ with catechols. Complexes **8**−**10**, possessing cofacial, metal-free SALPHEN-catecholate ligands, have been characterized by FAB− mass spectroscopy and elemental analysis. On the basis of (a) spectrocopic and analytical characterization and (b) the crystal structure of $(Bu_4N)_2[Mo_2O_5(Cu(EtO_2H_2SALPHEN\text{-}(O)_2))_2]$ (a metalated example of **10**), which shows the catecholate ligands in an η^2,μ-coordination mode, it is reasonable to conclude that the general, cofacial bis(catecholate) arrangement is a common structural feature in **8**−**10** as well.

As a matter of convenience, metal ions are introduced to the SALPHEN cavities of complexes **8**−**10** after binding the SALPHEN-catecholates to the $[Mo_2O_5]^{2+}$ bridge. This order is advantageous for the following reasons: (a) The unbound SALPHEN-catechol complexes, in some cases unavailable in high yields, are inconvenient for use as starting materials due to low solubility in organic solvents of low polarity. (b) Coordination of the catecholate functionality to the Mo atom of the $[Mo_2O_5]^{2+}$ core "blocks" the bidentate catecholate unit and ensures the formation of exclusively endocyclic derivatives. The syntheses of complexes $(Bu_4N)_2[Mo_2O_5(M^{II}(^tBu_4SALPHEN\text{-}(O)_2))_2]$ (M = Fe (**12**), Co (**14**), Ni (**16**), or Cu (**18**)) and $(Bu_4N)_2[Mo_2O_5(M^{II}(EtO_2H_2SALPHEN(O))_2)_2]$ (M = Mn (**11**), Fe (**13**), Co (**15**), Ni (**17**), or Cu (**19**)) were accomplished in near-quantitative yields by introducing the metal ions to the empty SALPHEN pockets in **9** and **10** using the metal(II) acetates or chlorides (Figure 4). Metalated derivatives of **8** tended to form oils, perhaps due to the lack of bulky substituents protecting the phenolic oxygens from exocyclic interactions with

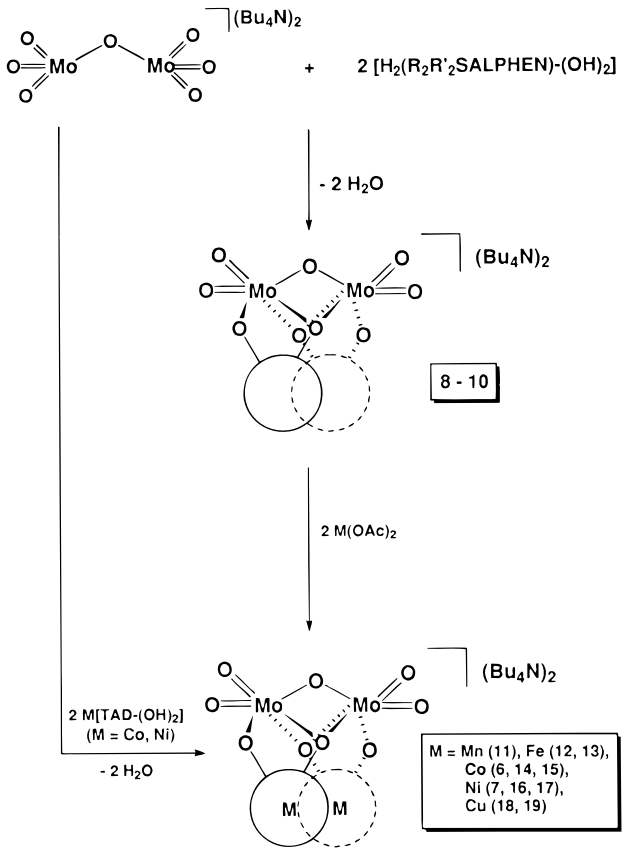

Figure 4. General reactions leading to the complexes **6**−**19**. The macrocyclic or SALPHEN portions of the catecholate ligands are depicted as circles, and the numbers represent various derivatives of these complexes as described in the Experimental section.

solvent and/or metal ions, and were therefore not pursued. The derivatives **6**, **7**, and **11**−**19** consist of two metalated macrocyclic or SALPHEN ligands bridged by the $[Mo_2O_5]^{2+}$ core, as inferred from the structures of **7** and **19** (vide infra). Analytical, spectroscopic, and magnetic characterization of these complexes suggests that the metal(II) ions (Mn, Fe, Co, Ni, and Cu) are in an approximate square-planar environment, with no axial ligation. Attempts were made to obtain Ru(II) adducts of **9** and **10** using either $Ru_3(CO)_{12}$, $[Ru(DMF)_6](BF_4)_2$, or $Ru(PPh_3)_3Cl_2$ as sources of Ru(II). In all cases, clean products were not obtained.

Description of Structures. The crystal and molecular structures of **7** and **19** have been determined. In both structures, the tetrabutylammonium cations were severely disordered but satisfactorily modeled and will not be discussed further.[16] This disorder accounts in part for the somewhat large *R* values. Selected crystallographic data are provided in Table 1.

In the structures of **7** (Figure 5) and **19** (Figure 6), the catecholate subunits are cofacially oriented and the $[(MoO_2)_2(\mu\text{-}O)]^{2+}$ unit assumes a bridging mode, essentially identical to that observed in the structures of the $[Mo_2O_5(D^tBC)_2]^{2-}$ (**1**) and $[Mo_2O_5(catecholate)_2]^{2-}$ anions.[13,14a] The Mo(VI) ions in these complexes are bridged by a single oxygen atom (O1). Each molybdenum ion is further ligated by a bidentate catecholate and two oxo groups in a cis orientation. The bidentate catecholate ligand on one Mo atom is also bridged to the other Mo atom through one of the O atoms. The mutual donation of an electron pair from one Mo(catecholate) unit to the other completes octahedral coordination for both of the Mo atoms. The $\eta_1\text{-}O_1;\eta_1,\mu_2\text{-}O_2$ bridging mode of the catecholate oxygens accounts in part for the cofacial orientation of these ligands.

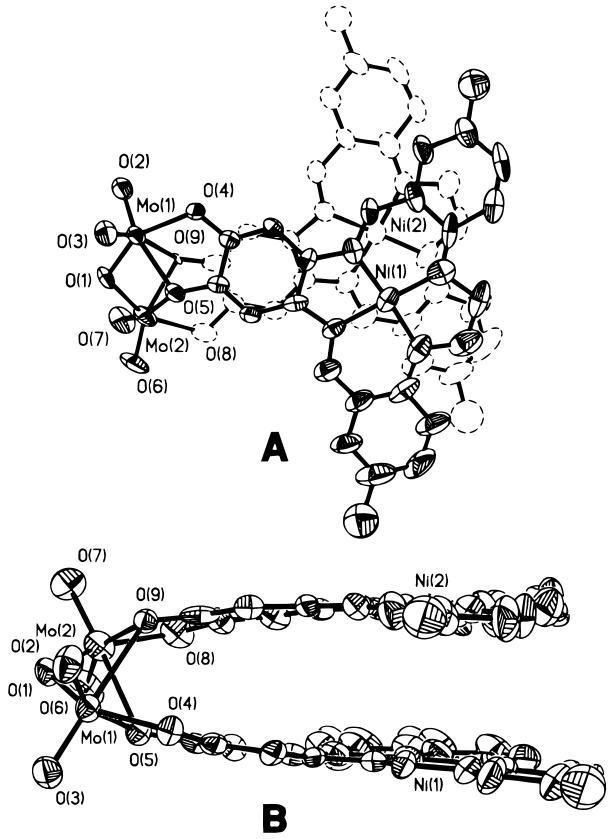

Figure 5. ORTEP plots (30% probability ellipsoids) showing two views of **7** (A) perpendicular and (B) parallel to the "planes" of the macrocycles.

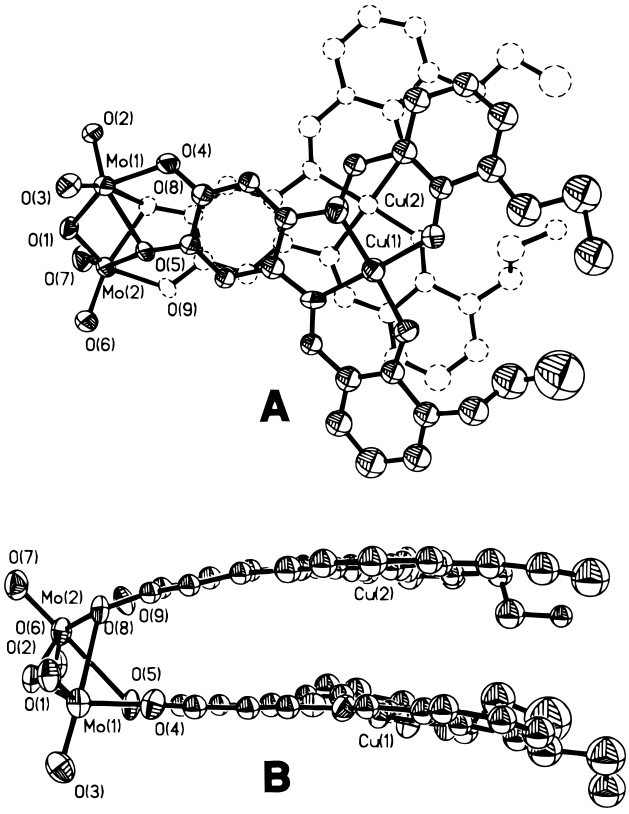

Figure 6. ORTEP plots (30% probability ellipsoids) showing two views of **19** (A) perpendicular and (B) parallel to the "planes" of the SALPHEN units.

Weak intramolecular $\pi-\pi$ interactions between phenyl rings also may favor the cofacial orientation of the catecholate ligands in the solid state. Such an orientation has been demonstrated for the $(pyH)_2[[(py)(Cl_4\text{-cat})MoO_2]_2(\mu\text{-O})]$[15] and $[[(SCN)(9,10\text{-phenanthroline})MoO_2]_2(\mu\text{-O})]$[25] complexes. In these molecules, the catecholate (or phenanthroline) ligands are strictly bidentate, with the sixth coordination site on each Mo ion occupied by a σ-base (either pyridine or thiocyanate) rather than a bridging O (or N) atom. In solution, relatively free rotation about the Mo−O−Mo unit undoubtedly occurs in these latter complexes, whereas the cofacial orientation of the catecholate ligands in molecules such as **1** is probably more rigid. The characterization of complexes such as $(pyH)_2[[(py)(Cl_4\text{-cat})MoO_2]_2(\mu\text{-O})]$ and $[[(SCN)(9,10\text{-phenanthroline})MoO_2]_2(\mu\text{-O})]$ suggest that, in the presence of suitable ligands, the bridging mode of the catecholate oxygen in molecules such as **1** may be disrupted. In such a case the inter-catecholate distance increases as the Mo−O−Mo angle opens up (vide infra).

Table 2 provides a comparison of bond distances and angles for the $[(MoO_2)_2(\mu\text{-O})]^{2+}$ bridge unit in **1**,[14a] **7**, **19**, $[[(9,10\text{-phenanthrenequinone})MoO_2]_2(\mu\text{-O})]$[15] (**A**), $(pyH)_2[[(py)(Cl_4\text{-cat})MoO_2]_2(\mu\text{-O})]$[19] (**B**), and $[[(SCN)(9,10\text{-phenanthroline})MoO_2]_2(\mu\text{-O})]$[25] (**C**). Mo(1)--Mo(2) distances at 3.179(2) Å in **7** and 3.237(4) Å in **19** are slightly longer than those reported in **1** (3.132(4) Å), $[Mo_2O_5(\text{catecholate})_2]^{2-}$ (3.13(1) Å) and $[(9,10\text{-phenanthrenequinone})MoO_2]_2(\mu\text{-O})]$ (3.160(2) Å) but as much as 0.6 Å shorter than the corresponding distances observed in $(pyH)_2[[(py)(Cl_4\text{-cat})MoO_2]_2(\mu\text{-O})]$ and $[[(SCN)(9,10\text{-phenanthroline})MoO_2]_2(\mu\text{-O})]$. This increased Mo(1)--Mo(2) separation in **B** and **C** results in Mo(1)−O(1)−Mo(2) angles that are closer to being linear (168.7(4) and 162.7(2)°, respectively). The corresponding Mo(1)−O(1)−Mo(2) angles in **7** (112.1(3)°) and **19** (116.2(6)°) are approximately 50° more acute than in **B** and **C** but are similar to those in **1** (109.4(4)°) and **A** (112.7(2)°). In similar molecules that (a) lack a bridging oxygen atom from a catecholate moiety, (b) lack phenyl rings that contribute to $\pi-\pi$ interactions, and (c) contain somewhat bulkier ligands, the Mo−O1−Mo angles are essentially linear.[24,26,27] This comparison of the solid-state structures of a number of molecules with the $[(MoO_2)_2(\mu\text{-O})]^{2+}$ bridge unit suggests that the bridging oxygen atom acts as a "hinge", allowing the Mo--Mo distance to change as the Mo−O(1)−Mo "bite" changes.

The macrocyclic subunits in **7** are nearly planar,[29] with rms deviations for all atoms of 0.110 and 0.144 Å, respectively. The angle between these planes is 6.5(2)°, which is small compared to the angle reported between the phenyl rings in **1** at 50.0(4)°, which may be due in large part to the bulky *tert*-butyl substituents in the latter. For comparison, the same angle in **A** is 19.3(3)°. The SALPHEN subunits in **19** define a dihedral angle of 9.7(1)° and are slightly puckered with rms deviations from the best planes[30] of 0.165 and 0.137 Å.

The intramolecular Ni(1)--Ni(2) distance in **7** is 3.938 Å, and the corresponding Cu(1)--Cu(2) distance in **19** is 4.110 Å. These distances are within the range reported for a variety of cofacial metalated porphyrin systems, from 3.417 Å in Co_2-(FTF4)[31] to 6.33 Å in Cu_2(FTF6).[32] The bis(Co−porphyrin) derivatives are catalysts in the reduction of O_2 to H_2O. The similar M--M spacing in the macrocyclic and SALPHEN

(29) For ligands A and B of **7**, the atoms with the largest deviation from planarity are O(4) (0.308(8) Å) and O(8) (0.352(8) Å), respectively.
(30) For ligands A and B of **19**, the atoms with the largest deviation from planarity are C(12) (0.39(2) Å) and O(8) (0.30(1) Å), respectively.
(31) Kim, K.; Collman, J. P.; Ibers, J. A. *J. Am. Chem. Soc.* **1988**, *110*, 4242. FTF4 represents the "face-to-face" porphyrins linked by two 4-atom amide bridges.

Table 2. Comparison of the Average Bond Lengths (Å) and Angles (deg) in Molecules That Contain the $[Mo_2O_5]^{2+}$ Core

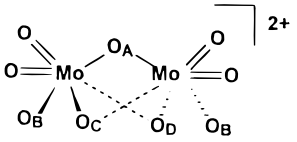

	1	7	19	A[a]	B[b]	C[c]
Mo═O	1.696(10)	1.704(9)	1.694(13)	1.686(5)	1.712(7)	1.690(5)
Mo−O_A	1.191(9)	1.916(8)	1.907(11)	1.898(5)	1.895(8)	1.875(4)
Mo−O_B	1.977(9)	2.007(8)	1.948(11)	2.041(14)	2.094(7)	
Mo−$O_{C(D)}$	2.156(9)	2.153(7)	2.172(11)	2.242(5)	2.165(7)	
Mo−$O_{C(D)}$ (bridge)	2.385(8)	2.538(8)	2.644(13)	2.495(5)	2.165(7)	
Mo--Mo	3.132(4)	3.179(2)	3.237(4)	3.160(2)	3.77[d]	3.70[d]
Mo−O_A−Mo	109.4(4)	112.1(3)	116.2(6)	112.7(2)	168.7(4)	162.7(20
O_C−Mo−O_D	71.5(3)	69.3(3)	68.2(5)	67.8(1)		
O_A−Mo−O_B	146.4(2)	147.9(3)	146.3(5)	142.1(2)	92.0(3)	
O_A−Mo−O_C	74.5(2)	77.5(3)	77.8(3)	76.9(2)	91.3(3)	
O_A−Mo−O_D	69.2(3)	68.2(3)	66.5(4)	70.7(2)		
O_B−Mo−O_C	75.8(4)	76.7(3)	76.5(4)	73.9(2)	74.3(3)	
O_B−Mo−O_D	86.8(3)	85.1(3)	84.0(4)	76.1(2)		
Mo−O_C−Mo, Mo−O_D−Mo	87.1(3)	84.9(3)	87.0(4)	83.5(1)		

[a] [[(9,10-Phenanthrenequinone)MoO_2]$_2$(μ-O)]. [b] (pyH)$_2$[[(py)(Cl_4-cat)MoO_2]$_2$(μ-O)]. [c] [[(SCN)(9,10-phenanthroline)MoO_2]$_2$(μ-O)]. [d] Calculated value.

derivatives suggests the potential of the latter to at least bind and perhaps activate O_2 in a similar manner (vide infra). The lateral displacement of Ni(1) relative to Ni(2) at 1.60 Å in **7** compares with similar "lateral slip" values for Ni_2(DPA) (2.40 Å),[33] Cu_2(DPB) (1.60 Å),[33] and Co_2(DPB) (1.57 Å).[34] The approximate "lateral slip" between the Cu atoms in **19** is only 0.6 Å.

In **4**, the average Ni−N distance in the macrocyclic unit is 1.85(1) Å, similar to that observed in both the uncomplexed catechol and in catecholato/metal complexes.[1,3] Likewise, the average Cu−N and Cu−O distances in the SALPHEN unit of **19** (1.93(1) and 1.88(1) Å, respectively) are unexceptional compared with those of a recently reported Cu(SALPHEN) structure.[35] Additional metric features of these ligands are not extraordinary and will not be discussed further. Only a brief listing of structural data is provided in Table 2. A complete listing of bond distances and angles, as well as other crystallographic data, has appeared previously.[16]

Mixed-Catecholate Complexes. Due to the differences in pK_a's associated with the various catechol ligands employed in this study, it appeared likely that mixed catecholate species could be isolated from the reaction of **1** (containing the most basic catecholate ligand) with only 1 equiv of a more acidic catechol. This was initially investigated using Cl_4-catechol. Slow addition of a THF solution of Cl_4-catechol to a solution of **1** in CH_2Cl_2 led exclusively to isolation of the mixed-catecholate complex (**4**), as indicated by its mass spectrum and unique electronic spectrum.

Initial investigations using the [H_2(^{t}Bu_4SALPHEN(OH)$_2$)] catechol suggested that the mixed-catecholate derivative (Bu_4N)$_2$[Mo_2O_5(D^{t}BC)(H_2(^{t}Bu_4SALPHEN(O)$_2$))] (**20**) could be isolated pure in good yield by selective recrystallization. The ^{1}H NMR spectrum of this compound is unique and shows one of the ring protons on D^{t}BC significantly shifted from those in **1** (6.70 ppm in **20** compared to 6.53 ppm in **1**). The electronic spectrum of **20** (Table 3) is also unique and not merely a mixture of **1** and **9**. The electronic absorptions in the spectrum of **20** show a bathochromic shift relative to **9**. While FAB− mass spectral analysis were inconclusive, electron-spray (ES) mass spectroscopy proved useful in characterizing these derivatives (vide infra).

Introduction of metal ions to the SALPHEN cavity of **20** was accomplished by reaction of **20** with 1 equiv of metal(II) acetate (Figure 7). The same products could be obtained by the direct reaction of **1** with M(^{t}Bu_4SALPHEN(OH)$_2$) (M = Co^{II} or Ni^{II}). Crystalline, analytically pure materials were isolated in all cases. Electron spray (ES−) mass spectroscopy showed a mass peak corresonding to [(Bu_4N)[Mo_2O_5(D^{t}BC)(M^{II}(^{t}Bu_4SALPHEN-(O)$_2$))]]$^-$ (M = Co (**21**), Ni (**22**), Fe (**23**), or Cu (**24**)) and no indications of the presence of **1** or **9**. Additionally, the electronic spectra for **21** and **22** are unique and bathochromically shifted by comparison to the bis(metalated) derivatives, similar to the trend observed for **20** (vide infra). The electronic spectra obtained for **23** and **24** were also unique with regard to the relative intensities of the absorbances but were not similarly shifted. The magnetic data obtained at 5 K were consistent with that typically observed for simple M^{II}SALEN derivatives, although values for μ_{eff}^{corr} were somewhat high at 300 K (vide infra).

The synthesis of **21**−**24** suggested a route into the synthesis of mixed-metal derivatives. These products would be desirable both for the investigation of potentially interesting spectroscopic properties and for the synthesis of site-specific/donor-atom-specific interactions that may lead to the activation of small molecules (N_2, CN^-, CO, etc.). However, the second 3,5-di-*tert*-butylcatecholate ligand could not be replaced by reacting **21**−**24** with a second 1 equivalent of M(^{t}Bu_4SALPHEN(OH)$_2$) (M = H_2, Co^{II}, or Ni^{II}), perhaps for steric reasons. Reactions of **22** with the less bulky H_2(EtO$_2$$H_2$SALPHEN(OH)$_2$) led to a mixture of products as evidenced from the mass spectrum (showing unreacted **22** and the products **10**, **16**, and the desired mixed-catecholate product) and the isolation of the free catechol Ni(^{t}Bu_4SALPHEN(OH)$_2$). The lack of sufficiently different

(32) Collman, J. P.; Chong, A. O.; Jameson, G. B.; Oakley, R. T.; Rose, E.; Schmittou, E. R.; Ibers, J. A. *J. Am. Chem. Soc.* **1981**, *103*, 516. FTF6 refers to two "face-to-face" porphyrins linked by two 6-atom amide bridges.

(33) See ref 5a. DPA refers to a cofacial diporphyrin system linked by an anthracene spacer. DPB refers to cofacial diporphyrins with a biphenylene spacer.

(34) Collman, J. P.; Hutchison, J. E.; Lopez, M. A.; Tabard, A.; Guilard, R.; Seok, W. K.; Ibers, J. A.; L'Her, M. *J. Am. Chem. Soc.* **1992**, *114*, 9869.

(35) Suresh, E.; Bhadbhade, M. M.; Srinivas, D. *Polyhedron* **1996**, *15*, 4133.

Table 3. Electronic Absorptions (800−250 nm) for Complexes **1**−**35**

complex	wavelength, nm ($10^{-4}\epsilon$, M^{-1} cm^{-1})	complex	wavelength, nm ($10^{-4}\epsilon$, M^{-1} cm^{-1})
1	333 (sh), 285 (1.1)	**19**	474 (sh), 417 (5.5), 395 (sh), 328 (4.7), 307 (sh)
2	303 (sh), 250 (sh)	**20**	426 (3.2), 353 (3.8), 258 (sh)
3	408 (sh), 327 (sh), 278 (sh)	**21**	480 (sh), 432 (3.7), 414 (sh), 331 (2.5)
4	303 (sh), 254 (sh)	**22**	474 (sh), 449 (4.1), 380 (3.5), 327 (3.1), 261 (8.2)
5	506 (5.2)	**23**	440 (sh), 407 (3.9), 329 (4.4), 297 (4.5)
6	655 (1.2), 548 (sh), 479 (sh), 434 (5.1), 309 (4.5), 296 (4.5), 250 (sh)	**24**	508 (sh), 455 (sh), 435 (5.6), 326 (3.1), 273 (4.9)
7	655 (1.2), 566 (sh), 426 (5.1), 394 (sh), 298 (7.8)	**25**	492 (sh), 390 (sh), 347 (4.5), 280 (sh), 265 (5.1)
8	419 (sh), 341 (4.0), 268 (5.9), 261 (6.4), 257 (sh)	**26**	514 (sh), 444 (2.8), 429 (sh), 403 (sh), 319 (sh), 274 (5.6)
9	419 (sh), 389 (3.7), 346 (4.1), 263 (5.3)	**27**	488 (sh), 414 (sh), 384 (3.9), 371 (sh), 305 (3.0)
10	423 (sh), 372 (sh), 332 (4.0), 275 (5.4)	**28**	342 (sh), 312 (sh), 300, 256
11	460 (sh), 407 (6.6), 320 (6.1)	**29**	456 (sh), 419, 341
12	441 (sh), 406 (6.1), 325 (6.3), 293 (6.1)	**30**	468 (sh), 406 (sh), 388, 368 (sh), 323, 256
13	455 (sh), 400 (5.4), 322 (6.1), 302 (sh)	**31**	472 (sh), 440 (sh), 406 (sh), 392 (5.2), 326 (4.1), 304 (sh), 258 (9.7)
14	474 (sh), 409 (7.2), 321 (5.1)	**32**	472 (sh), 440 (sh), 406 (sh), 392 (5.2), 326 (4.1), 304 (sh), 258 (9.7)
15	412 (7.4), 327 (6.3)	**33**	366 (2.3), 316 (sh), 273 (sh)
16	498 (sh), 472 (sh), 425 (sh), 397 (sh), 384 (5.9), 369 (sh), 321 (4.1), 314 (sh), 263 (11.0)	**34**	437 (sh), 359 (sh), 320 (7.1), 309 (sh)
17	474 (sh), 432 (sh), 389 (5.6), 323 (4.3), 301 (sh), 292 (sh), 256 (10.0)	**35**	451 (sh), 365 (sh), 320 (9.4), 306 (sh)
18	500 (sh), 456 (sh), 426 (8.0), 388 (sh), 320 (5.2), 268 (sh)		

Table 4. Magnetic Moments/Paramagnetic Subunit (M^{n+}) and Mossbauer Parameters[a] for Selected Complexes with Magnetic Moments/Complex Provided in Parentheses Where Appropriate

complex	μ_{eff}^{corr}/M^{n+}, (300 K)	μ_{eff}^{corr}/M^{n+}, (5 K)	typical[b] μ_{eff}^{corr}/M^{n+}, μ_B (300 K)	δ, mm/s	QS, mm/s
11	6.24 (8.82)	3.44 (4.86)	5.3−6.0 (Mn^{II})		
12	4.81 (6.76)	3.85 (5.44)	4.7−4.9 (Fe^{II})		
13	4.85 (6.86)	3.62 (5.12)			
23	5.06	4.69			
34	2.94 (4.16)	1.21 (1.71)	1.8−1.9/Fe^{III} in $[(Fe^{III})_2(\mu\text{-O})]$[c]	0.43	0.81
35	3.86 (5.45)	2.60 (3.67)	2.1−2.2/Fe^{III} in $[(Fe^{III})_2(\mu\text{-S})]$[4]	0.42	0.69
6	2.37 (3.30)	1.47 (2.08)	2.2−2.7 (Co^{II})		
14	2.58 (3.65)	1.67 (2.37)			
15	2.86 (4.04)	1.49 (2.11) (4 K)			
21	3.02	1.86			
26	2.0 (3.39)	1.64 (2.32)			
29	2.04 (2.88)	1.48 (2.10)			
18	2.19 (3.10)	1.88 (2.68)	1.8−2.0 (Cu^{II})		
19	2.89 (4.09)	1.75 (2.48) (4 K)			
24	2.68	1.83			
30	2.46 (3.49)	1.85 (2.62)	1.7−2.0 (semiquinone)		
32	2.41 (3.41)	1.56 (2.21)			

[a] Values reported vs Fe at 77 K. [b] See ref 36, unless noted otherwise. [c] See ref 38. [d] See ref 41.

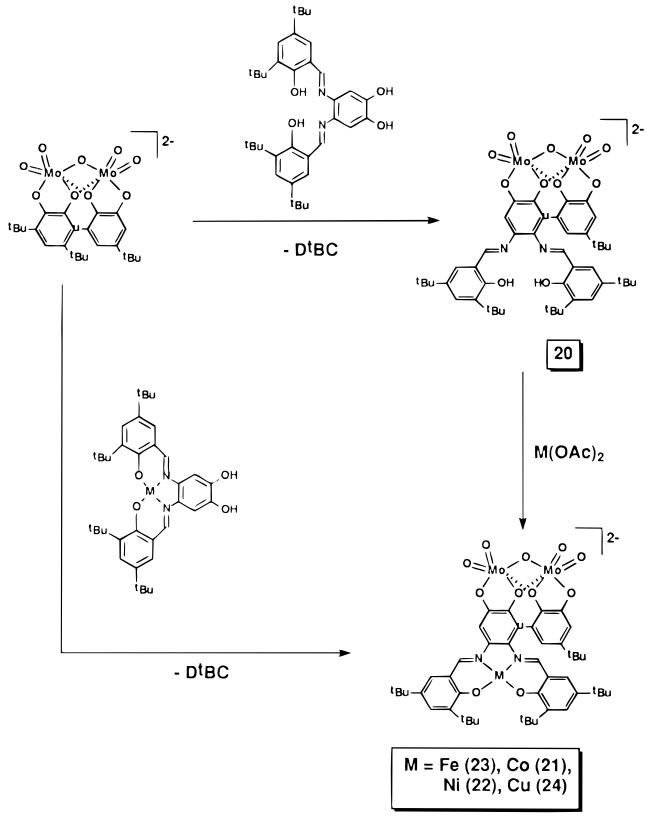

Figure 7. Synthesis of the mixed catecholate/SALPHEN-catecholate complexes **20**−**24**.

solubility characteristics between these products precluded isolation of the pure mixed-catecholate product. The reaction of $[Mo_2O_7]^{2-}$ with 1 equiv each of Ni(TAD(OH)$_2$) and H_2(^{t}Bu$_4$-SALPHEN(OH)$_2$) was performed in hopes of isolating a statistical mixture of products (i.e., a 50% yield of the mixed-catecholate complex) that *could* be isolated on the basis of

differential solubility. However, a 50% yield each of **7** and **9** was obtained. This implies that either none of the mixed-catecholate product formed initially or, more likely, the catecholates can dissociate from the $[Mo_2O_5]^{2+}$ core in solution and **7** slowly precipitates from solution as it forms. This catecholate lability is supported by mass spectral results. The mass spectrum (ES−) obtained on an CH_3CN solution of a mixture of pure **9** and **10** showed a very intense mass peak corresponding to the mixed-catecholate products as well as peaks corresponding to **9** and **10**.

Synthesis of Bis(semiquinone) Derivatives. There are three reported compounds that contain cofacial semiquinone ligands that are bridged by at least one $[Mo_2O_5]^{2+}$ moiety. The first is the neutral [[(9,10-phenanthrenesemiquinone)MoO_2]$_2$(μ-O)], synthesized from the reaction of $Mo(CO)_6$ with 9,10-phenanthrenequinone.[15] This molecule is reported to be diamagnetic, with the semiquinone coupled antiferromagnetically either through $\pi-\pi$ interactions between the closely spaced phenyl rings or through the Mo_2O_2 ring formed by the bridging oxygen atoms. Another example is the $[(Mo_2O_5)_2(C_6H_2O_4)_2]^{2-}$ complex, which contains two semiquinone ligands and is also diamagnetic.[23] Finally, $[(Mo_2O_5)_3(C_6O_6)_2]^{3-}$, which by overall charge considerations must contain only one semiquinone, displays an EPR spectrum with $g = 1.995$.[23] The latter two complexes were synthesized unexpectedly from di- and tetrahydroxybenzoquinone, respectively, with ligand disproportionation to radical species accounting for the incorporation of semiquinone ligands in these complexes. The $[Mo_2O_5(D^tBC)_2]$ dianion **1** was previously reported to undergo only one oxidation to form a semiquinone/catecholate complex, identified exclusively by EPR spectroscopy.[14a] A second oxidation reportedly resulted in complex degredation.

Low-quality cyclic voltamograms of the bis(SALPHEN-catecholate) dianions of **9**, **14** (in the absence of a coordinating solvent), and **16** showed two resolved quasireversible oxidation waves between 400 and 600 mV and 800−1000 mV, apparently from semiquinone and quinone formation, respectively, and will not be presented or discussed in detail. Nevertheless, an investigation into possibly obtaining chemically oxidized, bis(semiquinone) complexes was undertaken. The reaction of **9** with 2 equiv of $FcPF_6$ in CH_3CN led to a change in the color of the solution from deep orange to a yellow/green and formation of $Bu_4N(PF_6)$ that could be isolated in quantitative yield and characterized. The neutral bis(semiquinone) complex $[Mo_2O_5(H_2(^tBu_4SALPHENSQ(O)_2))_2]$ (**25**) was formulated on the basis of infrared spectroscopy, analytical results, and mass spectral analysis. The product could not be purified by chromatography using silica or alumina due to the highly polar Mo═O moieties. The solid is diamagnetic in the solid state, not unlike the simple semiquinone complexes described above. The EPR spectra of a solution of **25** (toluene or pyridine) routinely showed traces of semiquinone or, oddly, a signal with a *g* value and hyperfine splitting typical of Mo(V) and were independent of temperature (300−15 K). The combined integration of both of these signals, however, never amounted to more than 10% of that expected for the total anticipated concentration of organic radical, and consequently, the bulk of **25** is considered to be diamagnetic in solution as well. The apparent coupling of the semiquinone electrons supports a cofacial arrangement of the ligands.

The Co^{II} (**26**) and Ni^{II} (**27**) derivatives of **25** are synthesized in a similar manner and are characterized by elemental analysis and mass spectral data. Likewise, the $[Mo_2O_5(M(EtO_2H_2\text{-}SALPHENSQ(O)_2))_2]$ (M = H_2 (**28**), Co^{II} (**29**), or Ni^{II} (**30**)) derivatives were synthesized in a similar manner but are siginificantly less soluble than the *tert*-butyl-SALPHEN derivatives and hence precipitate out of CH_3CN as the oxidation proceeds. While elemental analysis suggests similar composition, mass spectral analysis was not performed on these derivatives due to the lack of solubility. The magnetic properties of **25**−**30** will be discussed in the next section.

General Spectroscopy and Physical Characterization. Infrared Spectroscopy. The infrared spectra of all complexes as listed in the Experimental Section show typical vibrations associated with the catecholate moiety, including relatively strong absorption peaks at 1480−1450 and 1280−1250 cm^{-1} that are assigned to the C═C and C−O bonds, respectively. The macrocyclic and SALPHEN derivatives also show a medium absorption peak associated with the C═N of the imine at approximately 1610−1590 cm^{-1}. The *cis*-MoO_2 moiety shows two very strong, relatively broad vibrations in the region 930−900 cm^{-1}, typical of the asymmetric and symmetric stretches in other such complexes.[14,15,19,23,24,26,27] Certain samples show a resolved third absorption peak in this region. Due to the abundance of absorptions in the 850−700 cm^{-1} region of the spectra from cations and the ligands, it is often difficult to unambiguously identify the vibrations associated with the Mo−O−Mo unit. The absorption peaks in the infrared spectra of the semiquinone complexes are somewhat broadened when compared to those of the catecholate precursors, but in general there is no dramatic shift associated with ligand oxidation. The far-IR spectra of these complexes cannot be assigned unambiguously and serve only as a means of recognitive characterization, since a particular class of compounds (i.e., complexes **8**−**10**) show similar far-IR spectra.

Electronic Spectroscopy. A list of absorbances and extinction coefficients is provided in Table 3. Spectra for the bis(metalated) complexes are typically dependent on the particular metal(II) but relatively independent of substituents on the SALPHEN ligand. They are nearly identical to those obtained for the uncomplexed catechols,[20] with small bathochromic shifts (∼10 nm) in the 300−500 nm region in the spectra of the catecholate complexes. A comparison between the Fe(II) derivatives **12** and **13** and those formulated as Fe(III)−(μ-Q)−Fe(III) derivatives (Q = O (**34**) or S (**35**)) shows a clear difference associated with the oxidation states and/or the bridging ligand in the electronic spectra, with the absorption bands shifting toward higher energy in the μ-Q derivatives.

In all cases, the electronic spectra of the metal-free bis(semiquinone) derivatives appear to show a hypsochromic shift when compared to the corresponding catecholate complexes. The latter are orange/red by comparison to the yellow/green semiquinone complexes. This trend is somewhat similar to what is observed with the simple catecholate systems, as complexes **1**−**3** are orange, while [[(9,10-phenanthrenequinone)MoO_2]$_2$-(μ-O)] is green.[15] The metal−ligand transitions in the metalated derivatives of both the SALPHEN-catecholate and the SALPHEN-semiquinone species dominate the electronic spectra. While there is no readily distinguishable difference between the spectra of **28**−**30** when compared to the catecholate precursors, the electronic spectra of the complexes **25**−**27** are unique. The differences between these classes of bis(semiquinone) derivatives may be due in part to the differences in the electron-withdrawing/-donating effects of the substituents on the phenyl rings of the respective SALPHEN-semiquinone ligands.

As mentioned previously, the electronic spectra of the "mixed" (D^tBC)(SALPHEN) derivatives show a red-shift in the major absorbances when compared to both the bis(SALPHEN)

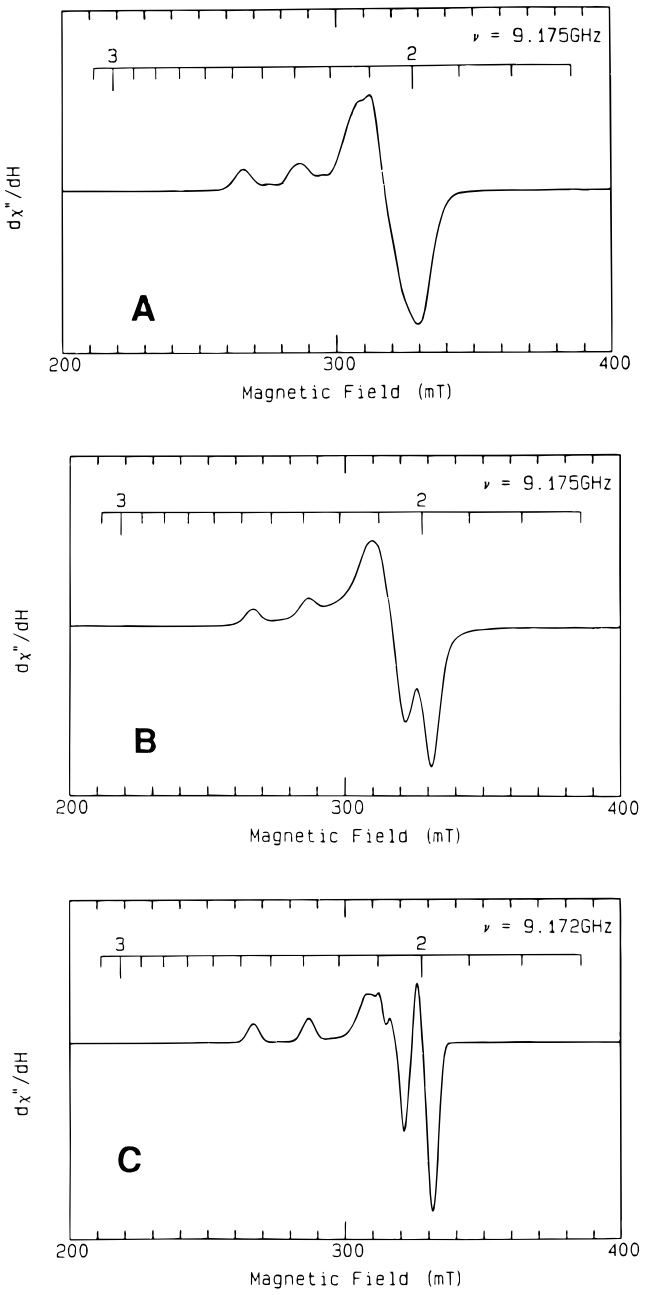

Figure 8. EPR spectra of (A) $[Mo_2O_5(Cu(^tBu_4SALPHEN(O)_2))_2]^{2-}$ (**18**), (B) $[Mo_2O_5(Cu(EtO_2H_2SALPHEN(O)_2))_2]^{2-}$ (**19**), and (C) $[Mo_2O_5(D^tBC)(Cu(^tBu_4SALPHEN(O)_2))]^{2-}$ (**24**), obtained from frozen CH_2Cl_2 solutions (100 K).

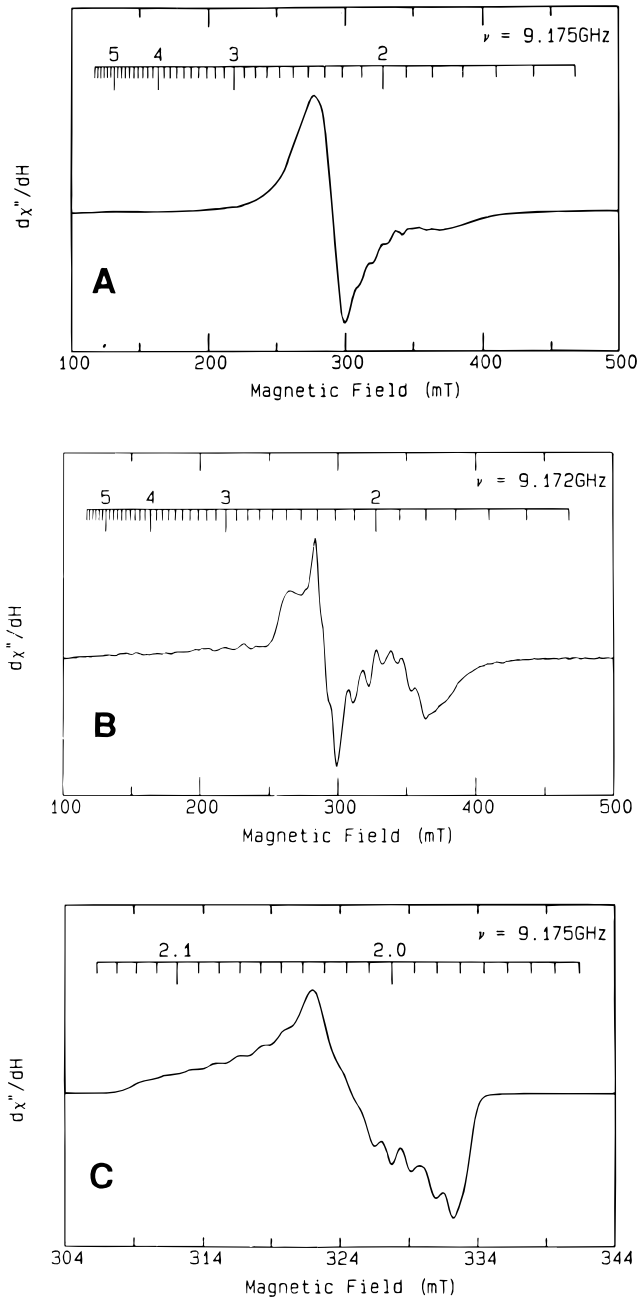

Figure 9. EPR spectra of (A) $[Mo_2O_5(Co^{II}(^tBu_4SALPHEN(O)_2))_2]^{2-}$ (**14**), (B) $[Mo_2O_5(D^tBC)(Co(^tBu_4SALPHEN(O)_2))]^{2-}$ (**21**), and (C) **21** in the presence of pyridine and O_2, with expanded scale to display hyperfine coupling. All spectra were obtained from frozen CH_2CN solutions (100 K).

and bis(D^tBC) complexes and the free catechols. This difference does not result from simply mixing equal amounts of the bis(SALPHEN) and bis(D^tBC) complexes and as such can be used for the identification of the mixed-catecholate derivatives.

Magnetic Properties and EPR Spectroscopy. In general, EPR spectra were obtained in frozen solutions (toluene, CH_2Cl_2, CH_3CN, or pyridine) at approximately 100 K for all derivatives of the semiquinone complexes and the Co and Cu derivatives of the catecholate complexes. The bis(Cu^{II}) complexes **18** and **19** (Figure 8A,B, respectively) and the bis(Co^{II}) catecholate complexes **14** and **15** (Figure 9A) display typical EPR spectra,[36] perhaps somewhat broadened and less resolved than the corresponding (M^{II}SALPHEN)(D^tBC) complexes **24** (M = Cu, Figure 8C) and **21** (M = Co, Figure 9B) and the uncomplexed SALPHEN catechol ligands.[20] This may be a consequence of weak interunit perturbations, particularly at lower temperatures. No half-field transitions were observed in these EPR spectra, however, which were observed in bis(Cu−porphyrin) complexes and used to estimate the Cu--Cu distances in the latter.[5a]

Table 4 lists the magnetic moments associated with the complexes at 300 and 5 K, with exceptions noted. All of the Ni^{II}−catecholate complexes were diamagnetic. As shown, the magnetic moments at 300 K for the Mn^{II}, Fe^{II}, Co^{II}, and Cu^{II} samples typically show a μ_{eff}^{corr}/M^{II} that is within the range reported for a variety of monomeric SALPHEN and SALEN derivatives, with evidence for weak antiferromagnetic coupling

(36) For example, see: Valko, M.; Klement, R.; Pelikan, P.; Boca, R.; Dlhan, L.; Bottcher, A.; Elias, H.; Muller, L. *J. Phys. Chem.* **1995**, *99*, 137.

at lower temperatures. The magnetic moments for all of the (M^{II}SALPHEN)(D^tBC) complexes are somewhat high at 300 K but are typical of monomeric M^{II}SALEN[37,38] at 5 K (vide supra).

The magnetic properties of the bis(semiquinone) derivatives [Mo_2O_5(M^{II}($R_2R'_2$SALPHENSQ(O)$_2$))$_2$] (R = R′ = *tert*-butyl, M = H_2 (**25**), Co (**26**), or Ni (**27**); R = EtO, R′ = H, M = H_2 (**28**), Co (**29**), or Ni (**30**)) were investigated as well. As mentioned, **25** is diamagnetic in the solid state and EPR silent in solution, not unlike what is observed in the simple [Mo_2O_5-(phenanthrenesemiquinone)$_2$] complex.[15] As expected, **27** is diamagnetic in the solid state and EPR silent in frozen solution (100 K), the square-planar Ni^{II} ions being diamagnetic. The magnetic moment of **26** in the solid state at 300 K (3.4 μ_B) is indicative of *two* unpaired spins. As many as *four* unpaired spins may be anticipated for **26**, composed of two low-spin Co^{II} ions and two semiquinone ligands. However, the two unpaired spins probably arise from the two low-spin Co^{II} ions assuming that (1) the semiquinone electrons couple as in the case of **25** and **27** and (2) the semiquinone electron *does not couple* to the Co^{II} unpaired electron. This latter point is substantiated by work with the well-characterized Co^{II}−SALPHEN-semiquinone complex [(bpy)$_2$Ru(Co^{II}($^tBu_4$SALPHENSQ(O)$_2$))]$^+$, which displays a magnetic moment (4.5 μ_B at 250 K) entirely consistent with *two uncoupled spins* (from the low-spin Co^{II} and semiquinone moieties) even at low temperature,[39] implying that the semiquinone and Co^{II} moieties do not "communicate" electronically. This observation is further substantiated by a simplified MO model suggesting that the frontier orbital for quinone-type moieties is *antibonding* with respect to C−O.[40] Indeed, the solid-state EPR spectrum of **26** showed features typical of Co^{II}, with only traces of organic radical. In frozen solution (toluene or pyridine, 100 K), however, **26** displayed no EPR signal. It is unlikely, particularly in noncoordinating solvent, that the intramolecular conversion of Co^{II}(SQ) to Co^{III}(catecholate) can occur, particularly in light of the above argument, although this may explain the observation that the sample is EPR silent. Intermolecular interactions in frozen solution are possible as well.

The metal-free derivatives **28** and [Mo_2O_5(D^tBSQ)(H_2($^tBu_4$-SALPHENSQ(O)$_2$))] (**33**), as well as the Co^{II} complex **29**, showed EPR and magnetic properties (Table 4) similar to **25** and **26**, respectively. The Ni^{II} complex **30**, however, while EPR silent in frozen pyridine solution (100 K) was paramagnetic in the solid state (μ_{eff}^{corr} = 3.4 μ_B at 300 K) and clearly showed an organic radical signal (g = 2.003) in the EPR spectrum of the solid state (100 K). In the absence of structural data, the differences between **27** and **30** are not understood currently, and if taken as a series, complex **30** seems to be the only example of a bis(semiquinone) complex with uncoupled electrons in the solid state. This may be due in part to the differences in electron-withdrawing/-accepting properties and the steric requirements of the substituents on the phenyl rings of the ligands.

Ligand Substitution Reactions. The solid-state structures of the anions in **1**, **7**, and **19** suggest that the inter-catecholate distance may depend on the extent to which the oxygen donor atoms of the chelating catecholate ligands bridge to the second Mo atom. The long (μ-O)−Mo bond at approximately 2.5 Å suggests that, in the presence of suitable ligands, the bridging

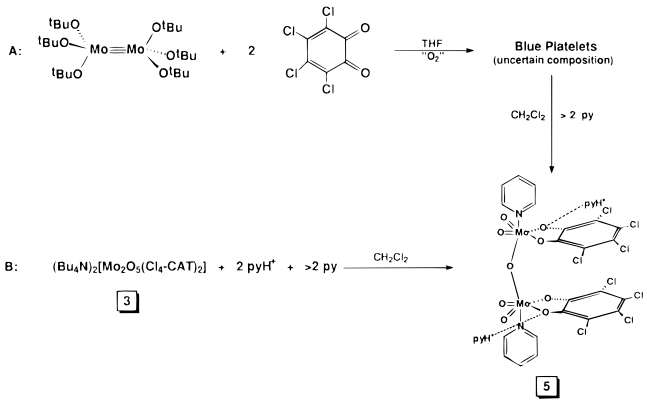

Figure 10. Synthesis of **5** from (A) a previously published procedure[19] and (B) the new synthesis from **3** as described in the text.

mode of the catecholate O may be disrupted by an external ligand "capping" the Mo atom. As discussed previously, the likelihood of changing the span of the Mo−O(1)−Mo angle between the two M^{II}-macrocyclic or M^{II}−SALPHEN subunits in the $[Mo_2O_5]^{2+}$ derivatives (and indirectly the M--M distance) represents an unusually attractive feature that may play a significant role in binding small substrate molecules between the metal sites of the macrocyclic or SALPHEN subunits. The strictly organic spacers employed in the bis(porphyrin) catalysts do not allow for this flexibility. This possibility was investigated by adding 2 equiv of various σ-bases to a solution of either complex **1** or **2** and investigating the resulting products by electronic and IR spectroscopy. The simple derivatives **1** and **2** were used for practical reasons. They are much more convenient to synthesize, and more importantly, the electronic spectra of these complexes are simple and unlike the bis-(SALPHEN-catechol) derivatives would readily show perturbations.

It was previously reported that the electronic spectrum of **1** showed new absorptions around 500 nm when strong-field ligands were added, such as CN^- or pyridine.[14b,c] This behavior was confirmed for CN^-, but the electronic spectra of **1** and **2** (and **8**−**10**) were unpurturbed in the presence of an excess of pyridine or imidazole (except for pyridine-/imidazole-based absorption at ∼ 300 nm). Weaker ligands such as SCN^- did not produce any changes in the electronic spectra, except for OH^- [303 (96 000), 246 (sh) nm (cm^{-1} M^{-1})] which very likely leads to Mo(VI) monomers. In all cases, however, attempts to isolated the base-ligated clusters by precipitation from solution were unsuccessful, and only the starting complex **1** or **2** and the tetraalkylammonium salt of the added ligand were isolated. Apparently, stronger ligands such as CN^- interact with the Mo atoms in the complex in solution, but the η^1-O_1;η^1,μ_2-O_2 ligating mode of the catecholate moiety persists in the solid state.

The reactivity of pyridine with complexes **1** and **2** was investigated further, in light of the observation that the latter of these compounds can be envisioned as a structural precursor to the (pyH)$_2$[[(Cl_4-cat)(py)MoO_2]$_2$(μ-O)] (**B**) complex which has been isolated and structurally characterized previously in an unrelated synthesis (Figure 10A).[19] In this molecule, the six-coordinate Mo(VI) ions in the bridging $[Mo_2O_5]^{2+}$ unit are each coordinated by a pyridine molecule rather than by a bridging catecholate oxygen lone pair, and the catecholate phenyl rings are still cofacially oriented. By comparison to **2**, the Mo−O−Mo angle in **B** opens to 168.7(4)° and the Mo−Mo separation is rather long at 3.77 Å.

Whereas the addition of 2 equiv of pyridine to (Bu_4N)$_2$-[Mo_2O_5(Cl_4-cat)$_2$] did not result in any change in the electronic

(37) Hobday, M. D.; Smith, T. D. *Coord. Chem. Rev.* **1972**, *9*, 311.
(38) Lewis, J.; Mabbs, F. E.; Weigold, H. *J. Chem. Soc. A* **1968**, 1699.
(39) Baumann, T. F.; Coucouvanis, D. Unpublished results.
(40) Vlcek, A., Jr. *Comments Inorg. Chem.* **1994**, *16*, 207.

spectrum, addition of pyH^+ (2 equiv, Figure 10B) results in a large bathochromic shift [303 (sh) → 506 nm (ϵ = 5200 M^{-1} cm^{-1})] and the isolated product (**5**) was found to be identical to **B**, based on a comparison of the analytical and spectroscopic properties previously reported.[19] Apparently the pyH^+ cations hydrogen bond to the catecholate oxygen atoms and "tie up" the lone pair used for bridging. This hydrogen-bonding interaction, evident in the crystal structure of **B**, is necessary for the structural change from **2** to **5**. Similar changes in the electronic spectra are observed upon addition of pyridine *and* pyridinium cations to solutions of **1**, **9** [358 (ϵ = 62 000 M^{-1} cm^{-1}), 393 (sh), 623 (ϵ = 37 000 M^{-1} cm^{-1}) nm], and **10** [347 (ϵ = 40 000 M^{-1} cm^{-1}), 388 (sh), 608 (ϵ = 20 000 M^{-1} cm^{-1}) nm]. This important H-bonding interaction is also demonstrated by the observation that a weaker acid (Et_3HN^+) does not result in a perturbation of the electronic spectrum of **2**, **9**, or **10**. Under identical reaction conditions, the electronic spectrum of **1** is similarly bathochromically shifted [344 (ϵ = 9000 M^{-1} cm^{-1}), 585 (ϵ = 17 000 M^{-1} cm^{-1}) nm] when either pyH^+ *or* Et_3HN^+ is present, as 3,5-di-*tert*-butylcatecholate is the most basic catecholate in the series.

The change in the catecholate binding mode from bridging η^1-O_1;η^1,μ_2-O_2 to chelating η^1-O_1,O_2 and the opening of the Mo−O−Mo angle that may accompany such a change impart flexibility to the possible distance between the catecholate subunits. Isolation of **5** was accomplished only due to the fact that **5** is insoluble in CH_2Cl_2. Attempting to "force" the product out of solution by layering with diethyl ether resulted in isolation of both **2** and **5** and some $pyH(PF_6)$. Even in the presence of added acid, an equilibrium must still exist between the complexes **2** and **5** in solution, indicating that the η^1-O_1;η^1,μ_2-O_2 ligating mode of the catecholate moiety is quite robust.

Given that the semiquinone ligands in complexes **25**−**30** are electron deficient when compared to the catecholate precursors, it seemed likely that the bridging mode of the η^1,μ_2-O semiquinone O would be significantly weakened, perhaps allowing for the "capping"of the Mo atoms with σ-bases in the absence of added acid. Dissolving complex **28** in neat pyridine does, in fact, result in a blue/violet solution (606, 349, 328 nm) in the *absence* of pyH^+, not unlike what is observed for the corresponding catecholate complex in the *presence* of pyH^+ (vide supra). However, dilution of this solution with any organic solvent, including DMF, results in a conversion back to the electronic spectrum characteristic of **28**.

Due to the relative insolubility of complexes **28**−**30**, a driving force for capping of the Mo atoms may result from the reaction of the bis(semiquinone) complexes with anions, which would result in a dianionic complex that would presumably be more soluble. Reaction of **30** with 2 equiv of $Et_4N(X)$ ($X = SCN^-$ or CN^-) in $MeNO_2/CH_3CN$ led to rapid dissolution of the starting material. Addition of diethyl ether resulted in the separation of red crystals (poor diffraction quality) that by infrared spectroscopy contained bound SCN^- (ν_{SCN} = 2085 cm^{-1}, indicative of N coordination) or CN^- (ν_{CN} = 2170, 2118 cm^{-1}) and by analysis suggested the formation of $(Et_4N)_2[[(X)(Ni(EtO_2H_2SALPHENSQ(O)_2))MoO_2]_2(\mu\text{-}O)]$ ($X = SCN^-$, **31**, or CN^-, **32**), Mo-capped derivatives of **30** where the $Mo-O_{catecholate}$ bridging interaction has presumably been broken. The electronic spectra and magnetic properties of **31** and **32** are indistinguishable from those of **30**. However, in the absence of a crystal structure, the exact orientation of the SALPHEN subunits cannot be unambiguously defined. It is possible that, in the solid state, a structure not unlike that observed for $[[(SCN)(9,10\text{-phenanthroline})MoO_2]_2(\mu\text{-}O)]$ is present. Suprisingly, the reaction of **27** with SCN^- did not lead to the expected product but instead resulted in isolation of unreacted $Et_4N(SCN)$. The difference in behavior between **27** and **30** in the presence of SCN^- may be due to both the extreme solubility of **27** in most organic solvents and the differences in SALPHEN ring substituents. The four *tert*-butyl groups on the SALPHEN units of **27** may donate enough electron density to the catecholate O to increase the strength of the $Mo-O_{catecholate}$ bridging interaction.

Single-Atom Bridged Complexes. It was initially observed that the electronic spectra of the bis(Fe^{II}) derivatives **12** and **13** changed noticeably on exposure to air, resulting in a slight hypsochromic shift of the primary metal-based electronic absorption. The pervasive occurrence of the unsupported $Fe^{III}-O-Fe^{III}$ moiety in a variety of systems, as in the case of [Fe(SALPHEN)]$_2$(μ-O)[41] and numerous other bis[Fe(macrocyclic)] systems,[42] suggested that similar μ-O dimers may form with the cofacially oriented Fe(SALPHEN) units in **12** and **13**. Isolation of the complex formed from bubbling O_2 through a solution of **13** yielded what is formulated as $(Bu_4N)_2[Mo_2O_5[(Fe(EtO_2H_2SALPHEN(O)_2))_2(\mu\text{-}O)]]$ (**34**) on the basis of elemental analysis, the change in the electronic spectrum, and mass spectral analysis. The Mossbauer spectrum, which clearly shows Fe(III) (Table 4), and the magnetic moment at room temperature, which is characteristic of strong antiferromagnetic coupling between two Fe^{III} ions (μ_{eff}^{corr} = 2.94 μ_B/Fe at 300 K, compared to 1.92 μ_B/Fe at 298 K for [(FeSALEN)$_2$(μ-O)][40] (Table 4), also support this formulation. A new spectral feature at ~590 cm^{-1} in the IR spectrum may be indicative of the Fe−O−Fe stretch but is difficult to assign unambiguously. Attempts at identifying the liberated equivalent of "O" were made by looking for oxidized products of THF, adamantane, or cyclohexene (all >50-fold excess relative to **34**) in separate experiments. However, no oxidized products were identified conclusively.

To distiguish between intra- vs intermolecular bridging O, an CH_3CN solution of $[Mo_2O_5(D^tBC)(Fe^{II}(^tBu_4SALPHEN(O)_2))]^{2-}$ (**23**) was similarly treated with O_2. After 4 h of exposure to air, only a very slight perturbation in the electronic spectrum was observed [440 (sh), 405 (35 000), 324 (43 000), 290 (45 000) nm (M^{-1} cm^{-1})], unlike that observed for **12** and **13** after exposure to air for only 5 min. A μ-O dimer resulting from the reaction of **23** with O_2 can *only* occur if an intermolecular Fe−O−Fe unit is formed. The apparent lack of μ-O dimer formation with **23** may be due to unfavorable steric interactions and suggests that **12** and **13** accommodate exclusively intramolecular O bridges upon reaction with O_2.

The unsupported sulfide-bridged complex [(FeSALEN)$_2$(μ-S)] has been synthesized by reaction of Na_2S[43] or $(Me_3Si)_2S$[44] with [(FeSALEN)$_2$(μ-O)] or from the reaction of elemental S with Fe(SALEN).[45] Reaction of **13** with BzSSSBz, which is known to oxidatively add sulfide to metal atoms,[46] yielded a product which is formulated as the μ-S complex **35**, $(Bu_4N)_2[Mo_2O_5[(Fe(EtO_2H_2SALPHEN(O)_2))_2(\mu\text{-}S)]]$ on the basis of (1) the Mossbauer spectrum, which clearly indicates exclusively Fe^{III} (Table 4), (2) the magnetic moment at 300 K

(41) Mukherjee, R. N.; Stack, T. D. P.; Holm, R. H. *J. Am. Chem. Soc.* **1988**, *110*, 1850 and references therein.
(42) Murray, K. S. *Coord. Chem. Rev.* **1974**, *12*, 1.
(43) Mitchell, P. C. H.; Parker, D. A. *J. Inorg. Nucl. Chem.* **1973**, *35*, 1385.
(44) Dorfman, J. R.; Girerd, J.-J.; Simhon, E. D.; Stack, T. D. P.; Holm, R. H. *Inorg. Chem.* **1984**, *23*, 4407.
(45) Floriani, C.; Fachinetti, G. *Gazz. Chim. Ital.* **1973**, *103*, 1317.
(46) Coucouvanis, D.; Swenson, D.; Stremple, P.; Baenziger, N. C. *J. Am. Chem. Soc.*, **1979**, *101*, 3392.

(3.86 μ_B/Fe), which is indicative of antiferromagnetic coupling between the two high-spin Fe^{III} ions, as reported for [(FeSALEN)$_2$(μ-S)] (2.1−2.2 μ_B/Fe at 290 K),[44] (3) the characteristic change in the electronic spectrum not unlike that observed for the μ-O complex **34** (Table 3), (4) the presence of a new weak absorption in the far-infrared spectrum at approximately 440 cm^{-1} which is likely due to the Fe−S−Fe unit, and (5) satisfactory elemental analysis. The byproduct BzSSBz was also identified in the supernatant by direct probe mass spectroscopy. Finally, the addition of excess PEt_3 to solutions of neat **35** led to (1) regeneration of the electronic spectrum characteristic of the bis-Fe^{II} complex **13** due to the reductive elimination of S^{2-} and (2) the isolation of S═PEt_3 (ν(P═S) = 536 cm^{-1}) and O═PEt_3 (ν(P═O) ≈ 1140 cm^{-1}), the latter undoubtedly arising from decomposition of the $[Mo_2O_5]^{2+}$ core.

Formation of an Apparent μ-O_2 Complex with Co^{II} Complexes. Since the initial observation in 1938 of the oxygen-carrying properties of Co^{II}SALEN,[47] a plethora of studies have been performed on the oxygenation of Co^{II}−Schiff base complexes.[48] Briefly, Co^{II}SALEN derivatives are oxygenated to form both 2:1 and 1:1 adducts in the presence of suitable axial bases (pyridine, DMF, imidazole) at low temperature (less than 15 °C). The 2:1 SALEN/O_2 derivatives are diamagnetic in both the solid state and in solution, while the 1:1 adducts are paramagnetic with a characteristic solution EPR spectrum showing an organic radical signal with an 8-line hyperfine splitting (usually $g_{||}$ and $g_\perp$) due to interaction of the unpaired spin with the $I = {}^7/_2$ Co nucleus. The structure of [(DMF)(CoSALEN)]$_2$(μ-O_2) displays[49] an O_2 molecule bridging two Co atoms, the latter of which are capped by DMF molecules. The Co--Co distance at approximately 4.2 Å and the O−O bond length (1.334(6) Å) suggest that the electronic structure of the dioxygen bridge is unique when compared to other structures with known peroxo or superoxo bridges. The molecule is diamagnetic, however, suggesting peroxo bridging between two Co^{III} atoms. In general, these unsupported μ-O_2 complexes can be deoxygenated under vacuum while warming at 80 °C or, in some cases, upon dilution with a noncoordinating solvent.

The EPR spectrum of a frozen CH_3CN solution (100 K) of $(Bu_4N)_2[Mo_2O_5(D^tBC)(M(^tBu_4SALPHEN(O)_2))]$ (**21**) is shown in Figure 9B and is typical of Co^{II}. Addition of a slight excess of pyridine to this solution undoubtedly results in coordination of pyridine to form a 5-coordinate, square-pyramidal Co^{II},[39,50] which upon exposure to O_2 displays an EPR signal (Figure 9C) typical of a Co^{III}−superoxo moiety, with 8-line hyperfine splitting pattern ($g_{||}$ and $g_\perp$) due to interaction of the unpaired electron on the superoxide (O_2^-) with the $I = {}^7/_2$ nucleus of Co. This observation could be due to either (a) oxygen binding on the "outside" of the cluster in the absence of intermolecular bridging, or b) oxygen binding on the "inside" of the pocket, protected from intermolecular bridging by the catecholate ligand. In the presence of pyridine, it is likely that Co is axially ligated by the solvent on the "outside" of the pocket for steric reasons, and therefore binding of O_2 on the "inside" of the pocket seems reasonable (Figure 11). Similar results also have been observed in the mixed-metal, bridged diporphyrin molecules [(L)(Co)(Pd)FTF4][8] and [(L)(Co)(InCl)DPA],[9] where the sterically bulky L = 1-*tert*-butyl-5-phenylimidazole was assumed to bind exclusively on the "outside" of the diporphyrinic cavity.

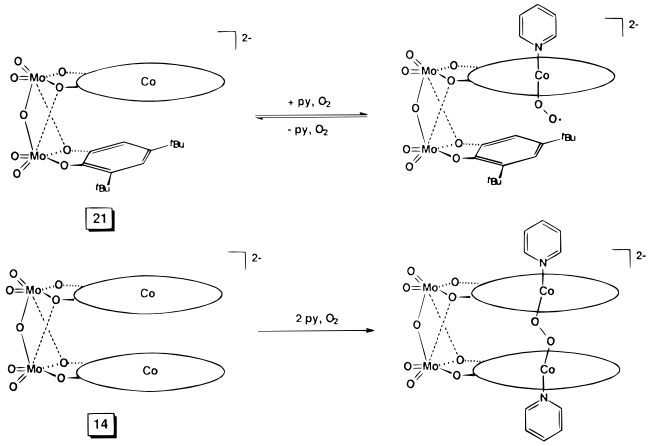

Figure 11. Proposed formation of O_2 adducts of $[Mo_2O_5(Co^{II}(^tBu_4SALPHEN(O)_2))_2]^{2-}$ (**14**) and $[Mo_2O_5(D^tBC)(Co^{II}(^tBu_4SALPHEN(O)_2))]^{2-}$ (**21**).

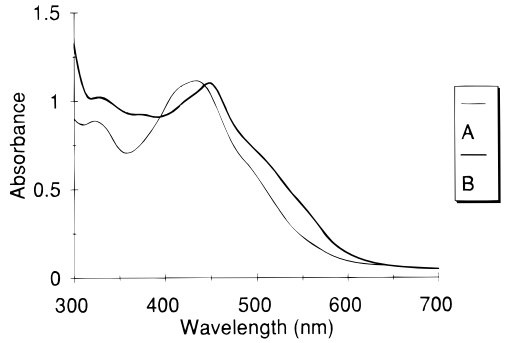

Figure 12. Electronic spectra obtained in CH_3CN/pyridine (20:1) solutions of (A) $[Mo_2O_5(D^tBC)(Co^{II}(^tBu_4SALPHEN(O)_2))]^{2-}$ (**21**) and (B) **21** in the presence of O_2.

The EPR results were further correlated with electronic spectroscopy. Figure 12A shows the electronic spectrum of pyridine-ligated **21**. Bubbling O_2 through this solution for approximately 5 min at room temperature resulted in the spectral change shown in Figure 12B, which consists of a shift of the primary absorbance by approximately 20 nm. The solvent from this oxygenated solution was removed *in vacuo*, and subsequently, the residue was heated at 80 °C under vacuum for approximately 30 min. Redissolving the residue in neat CH_3CN resulted in an electronic spectrum identical to that obtained in O_2-free solutions of **21** (i.e., Figure 12A). In the presence of additional pyridine, oxygenation of this solution again provided the electronic spectrum shown in Figure 12B. The observed changes in both the EPR and electronic spectra are therefore consistent with reversible O_2 binding to the Co atom in **21**, not unlike what is observed in simple Co^{II}SALEN systems.[48]

The spectroscopic results discussed above suggest that, for **21**, O_2 binds to the single Co^{II} ion (1) reversibly and (2) most likely on the "inside" of the pocket generated by the cofacial SALPHEN-catecholate and 3,5-D^{t}BC ligands. Under identical conditions, it seemed likely that $[Mo_2O_5(Co^{II}(R_2R'_2SALPHEN(O)_2))_2]^{2-}$ (**14**, R = R′ = *tert*-butyl; **15**, R = EtO, R′ = H) might also bind O_2 on the inside of the diSALPHEN pocket, resulting in a Co−O_2−Co bridge unit (Figure 11). Upon exposure to

(47) Tsumaki, T. *Bull. Chem. Soc. Jpn.* **1938**, *13*, 252.
(48) For example, see: (a) Floriani, C.; Calderazzo, F. *J. Chem. Soc. A* **1969**, 946. (b) Crumbliss, A. L.; Basolo, F. *J. Am. Chem. Soc.* **1970**, *92*, 55. (c) Ashmawy, F. M.; Issa, R. M.; Amer, S. A.; McAuliffe, C. A.; Parish, R. V. *J. Chem. Soc., Dalton Trans.* **1986**, 421. (d) Chen, D.; Martell, A. E. *Inorg. Chem.* **1987**, *26*, 1026. (e) Chen, D.; Martell, A. E.; Sun, Y. *Inorg. Chem.* **1989**, *28*, 2647. (f) Dzugan, S. J.; Busch, D. H. *Inorg. Chem.* **1990**, *29*, 2528, and references therein.
(49) Calligaris, M.; Nardin, G.; Radaccio, L.; Ripamonti, A. *J. Chem. Soc. A*, **1970**, 1069.
(50) Kennedy, B. J.; Fallon, G. D.; Gatehouse, B. M. K. C.; Murray, K. S. *Inorg. Chem.* **1984**, *23*, 580.

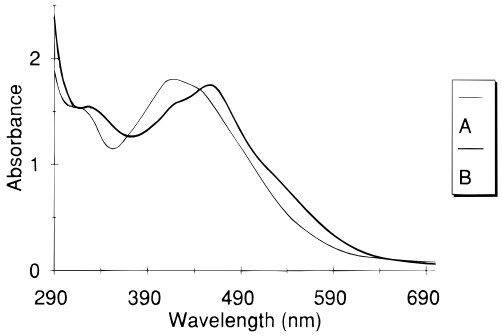

Figure 13. Electronic spectra obtained in CH_3CN/pyridine (20:1) solutions of (A) $[Mo_2O_5(Co^{II}(^tBu_4SALPHEN(O)_2))_2]^{2-}$ (**14**) and (B) **14** in the presence of O_2.

O_2, CH_3CN/pyridine solutions of **14** or **15** display the following spectroscopic changes: (1) The primary absorbance at 410 nm in the electronic spectrum shifts to 450 nm upon exposure to O_2 (Figure 13), not unlike the spectral change associated with oxygenated solutions of **21**. Unlike **21**, however, the spectral change associated with oxygenated **14** or **15** is *not* reversible under similar conditions. (2) Upon exposure to O_2, CH_3CN solutions of **14** in the presence of pyridine or DMF (both with and without pyH^+) become EPR silent (measured at 100 K), suggesting a $Co^{III}-O_2^{2-}-Co^{III}$ bridging unit which should be diamagnetic. (3) ES− mass spectral results obtained from oxygenated CH_3CN/pyridine solutions of **14** show mass peaks associated with $[(Bu_4N)[Mo_2O_5(Co^{II}(^tBu_4SALPHEN(O)_2))_2]]^-$ (1770.0 Da/e), pyridine-ligated $[(Bu_4N)[Mo_2O_5(pyCo^{II}(^tBu_4SALPHEN(O)_2))_2]]^-$ (1927.4 Da/e), and the dioxygen adduct $[(Bu_4N)[Mo_2O_5(pyCo^{II}(^tBu_4SALPHEN(O)_2))_2(\mu\text{-}O_2)]]^-$ (1960.6 Da/e). No mass peak associated with the monooxo-bridged complex was observed. These observations suggest that the two Co^{II} centers in **14** and **15** at close proximity may tightly "pinch" the O_2 molecule in the pocket, not unlike what was observed in the unsupported O_2-bridged $[(DMF)(CoSALEN)]_2(\mu\text{-}O_2)$[49] and proposed for $[(LCo)_2(\mu\text{-}O_2)FTF4]$.[8] Attempts at isolating analytically pure solid samples of this postulated μ-O_2 adduct have instead yielded a variety of apparent decomposition products, including uncomplexed Co^{II}SALPHEN.

Summary and Conclusions

The following points reiterate the principle results of this work.

(a) The new synthesis of **1** using $[Mo_2O_7]^{2-}$ was extended to the macrocyclic- and SALPHEN-catechols, leading to the supermolecular products **6**−**19**. The latter are composed of cofacially-oriented, catechol-functionalized macrocyclic and SALPHEN moieties bridged by the $[Mo_2O_5]^{2+}$ unit. On the basis of the crystal structures of **7** and **19**, the M^{II}--M^{II} intramolecular distances in **6** and **11**−**18** should be approximately 4 Å (M = Mn, Fe, Co, Ni, or Cu), as found for **7** and **19**.

The $[Mo_2O_5(Co^{II}(SALPHEN(O)_2))_2]^{2-}$complexes, conceptually and geometrically similar to the bis(Co^{II}−porphyrin) molecules, do not share similar unique physical properties.[51] The EPR spectra, room temperature magnetic moments, and the electronic spectra of the former complexes are not radically different form those of either the free Co^{II}−SALPHEN-catechols or "monomeric" Co^{II}−SALPHEN-catecholate complexes. While not thoroughly investigated due to poor quality, the cyclic voltamograms of these complexes do not suggest separate, distinct waves attributable to individual reductions or oxidations of the Co^{II} ions or individual ligand oxidations which one would expect if the two ions/ligands in the $[Mo_2O_5(Co^{II}(SALPHEN(O)_2))_2]^{2-}$complexes "communicated" electronically as is clearly present in the bis(Co^{II}−porphyrin) complexes. All of these observations suggest that there is little or no "cooperative effect" between the metal-containing SALPHEN subunits in these complexes, which may be due in part to either the lack of conjugation/aromaticity and/or the lack of strict planarity in the SALPHEN substituents.

(b) A series of "mixed-catecholate" derivatives **20**−**24** have been obtained from the reaction of **1** with 1 equiv of $M(^tBu_4SALPHEN(OH)_2)$ (M = H_2, Fe^{II}, Co^{II}, Ni^{II}, or Cu^{II}). Other mixed-catecholate and mixed-metal complexes cannot be readily isolated.

(c) Reaction of the bis(SALPHEN-catecholate) complexes with 2 equiv of oxidant (Fc^+) has led to the isolation of bis(SALPHEN-semiquinone) derivatives **25**−**30**.

(d) The ability of the SALPHEN-catecholate complexes to bind small ions or molecules in the "pocket" generated by the two cofacial SALPHEN moieties has been investigated. Included among these products are the μ-O derivative of **13** and apparent μ-O_2 derivatives of **14** and **15**, the latter of which have only been identified on the basis of spectroscopic data of the complexes generated in solution.

(e) The bridging interaction between the Mo atom and the O atom from the adjacent catecholate in molecules such as **1**−**19** can be disrupted in the presence of suitable "capping" ligands and pyH^+ in solution. The latter "ties up" a lone pair of electrons on the O atom through H-bonding, making the electrons unavailable for bridging. This property allows for the Mo--Mo distance, and indirectly the M^{II}--M^{II} distance, to increase.

The $[Mo_2O_5(SALPHEN\text{-}catecholate)_2]^{2-}$ complexes discussed in this paper have interesting geometric and reactivity properties, the latter being unobserved in bis(porphyrin) complexes. However, the former seem to lack unique physical properties. The apparent lack of intramolecular electronic "communication" in the bis(SALPHEN) derivatives may be due to the lack of conjugation/aromaticity of the SALPHEN subunit. Future work may involve the use of new ligands that are at least fully conjugated in order to observe seemingly important electronic effects in these inorganic complexes.

Acknowledgment. The support of this work by the National Science Foundation (Grant CHE-9307382) is gratefully acknowledged. We also thank Dr. N. Moon, Dr. W. R. Dunham, and Dr. T. F. Baumann for obtaining EPR spectra, Dr. R. Ogorzalek Loo for useful discussions regarding ES mass spectral results, and R. A. Reynolds III for generously providing $[M^{II}(TAD(OH)_2)]$ (M = Co, Ni).

Supporting Information Available: Text providing complete synthetic details, as well as elemental analysis and spectroscopic characterization data, for compounds **1**−**3**, **11**−**19,** and **24**−**30** (8 pages). Ordering information is given on any current masthead page.

IC9715916

(51) (a) Le Mest, Y.; Inisan, C.; Laouenan, A.; L'Her, M.; Talarmin, J.; El Khalifa, M.; Saillard, J.-Y. *J. Am. Chem. Soc.* **1997**, *119*, 6095. (b) Le Mest, Y.; L'Her, J. T.; Saillard, J.-Y. *Inorg. Chim. Acta* **1996**, *248*, 181. (c) Le Mest, Y.; L'Her, M.; Hendricks, N. H.; Kim, K.; Collman, J. P. *Inorg. Chem.* **1992**, *31*, 835.